IEEE Access
Multidisciplinary | Rapid Review | Open Access Journal

Received September 26, 2021, accepted October 1, 2021, date of publication October 4, 2021, date of current version October 19, 2021.

Digital Object Identifier 10.1109/ACCESS.2021.3117701

Reweighted Error Reducing Channel Estimator for QoS Enhancement in Wireless Nautical Radio Networks

OWOICHO E. IJIGA[1], (Member, IEEE), REZA MALEKIAN[1], (Senior Member, IEEE), AND UCHE A. K. CHUDE-OKONKWO[2], (Member, IEEE)

[1]Department of Electrical, Electronic and Computer Engineering, University of Pretoria, Pretoria 0002, South Africa
[2]Institute of Intelligent Systems, University of Johannesburg, Johannesburg 2092, South Africa

Corresponding authors: Owoicho E. Ijiga (owoicho.ijiga@gmail.com) and Reza Malekian (reza.malekian@up.ac.za)

This work was supported in part by the National Research Foundation/Research and Innovation Support and Advancement (NRF/RISA) Research Grant of South Africa, in part by the University of Pretoria Doctoral Research Grant and in part by the Centre for Connected Intelligence (CCI), Advanced Sensor Networks Research Group, University of Pretoria.

ABSTRACT Maritime explorations may suffer from unwanted situations such as delays, insecurity, congestions, and collisions, etc., which may arise from severe environmental conditions. Thus, there is a need to develop proper techniques that will improve the overall *quality of service* (QoS) of marine users. This work aims to address the limitations of wireless transmissions over maritime communication systems using channel estimation (CE) by designing and verifying the performances of two estimators named *inter-symbol interference/average noise reduction* (ISI/ANR) and *reweighted error-reducing* (RER) for aggrandizing the quality of nautical radio transmissions. To show that adopting accurate and stable CE methods can considerably increase the QoS requirements of marine networks, the performances of the proposed estimators are analysed in comparison to traditional methods under signal propagations assuming both line of sight (Rician) and Non-line of sight (Rayleigh) conditions. The adoption of a reweighting attractor in addition to the introduction of a variable leakage factor controlled log-sum penalty function to our proposed RER estimator provides additional stability for the estimation of oceanographic channels. Results obtained highlight that the proposed estimator demonstrates a performance gain of over 1 dB at a data rate of 100 bps under severe fading environments in comparison to the customary RLS technique. At an MSE of 10^{-2}, the RER method under slow fading channels show a performance gain of about 1 dB when compared to the traditional RLS method while similarly showing superiority gain of about 0.6 dB over RLS method assuming fast fading Rayleigh channel conditions.

INDEX TERMS Channel fading, Internet of Things, maritime networks, RER channel estimation.

I. INTRODUCTION

The paradigm of internet of things (IoT) can be described as a fascinating system of interconnected computing devices with crucial application scenarios in the fast emerging fifth generation (5G) networks and beyond [1]. This indispensable paradigm is essential in applications ranging from smart societies, industrial applications and security etc. In the industries, IoT can be deployed in sectors such as manufacturing, transportation, healthcare, smart energy and food production. Particularly, the maritime industry is faced with numerous binding constraints which may arise from either anthropogenic or naturogenic conditions like delivery and traffic clearance delays, environmental degradation (oil and toxic waste spillages), congestion control management, insecurity and inefficient road networks [2]. These maritime limitations can be mitigated by deploring the IoT in what is known as the internet of maritime things (IoMT), where sensors are positioned at strategic locations to enhance the monitoring of maritime environments in addition to the prevention of disaster occurrences. Nevertheless, the realization of IoMT is limited by factors such as wide area coverages, efficient

The associate editor coordinating the review of this manuscript and approving it for publication was Alessandro Pozzebon.

allocation/optimization of network resources, cost-effective communication, mobility management and secure signal transmission [3]. Consequently, reliable and high-speed devices with efficient data services are required to meet wide network coverage needs. Satellite communication are reliable communication systems that provide high network data rate applications in addition to wide area networks. Be that as it may, these communication systems are not cost effective. Hence, there is need for developing alternative cost-effective IoMT-based network technologies for improved operation of maritime activities which is considered in this research work.

Wireless communication within the marine environment is affected by severe environmental conditions such as extreme temperatures, deepwater waves, ship movements, inconsistent weather conditions including rain, snow and fogs etc. The seaside territories usually consist of constricted infrastructures that eventually overwhelm the quality of transmission between the ocean-going vessels and the outlying shore-positioned base station (BS) whereas, marine users (just like terrestrial users) require high-quality broadband communication services like ship rescue, voice and data services in addition to video monitoring services for the operations of maritime ministrations. To overcome these challenges, there is a need to design cost-effective and energy efficient network architectures and communication techniques that will eventually enhance the communication quality and extended signal coverages across ocean-water surroundings. More so, the IoMT-installed sensor networks are usually affordable (low cost) communication systems, which can be enacted in the development of perceptible cost-effective communication meshes in the nautical radio networks. However, the aggregated information to be propagated across the maritime channel will have traits such as low speed and low power, since the travelling sensor information will have low and weak transmission capabilities. As a result of the absence of carrier frequency signal transmission (or modulation) techniques and due to the limitations of the sensor-based networks such as low-speed transmissions, the transmitting cluster head (CH) information in an IoMT system will most likely experience severe effects of multipath propagation and fading. Because the sensor information deployed in maritime wireless communication networks transmit under low power conditions in an atmospheric condition that constitute a high possibility of multipath propagation and signal fading, robust and efficient channel estimation (CE) methods are consequently required to mitigate the unsolicited impacts and effects of these detrimental phenomena so that the communication quality and proficiency of pelagic networks can be substantially improved. Channel estimation is a useful communication technique that can be exploited for maritime explorations in the receivers of deep-sea networks. In this way, the effects of the communication channel on the transmitted packets can be understood and reasonably predicted for useful nautical decision-making procedures [4]. Motivated by these reasons, this paper proffers an IoT-based working solution to the challenges of network transmission and traffic management in the maritime environment by describing an IoT-enabled network architecture, where two CE techniques (named reweighted error-reducing (RER) CE and inter-symbol interference/ average noise reduction (ISI/ANR) CE) are carefully proposed and evaluated for improving the quality of service (QoS) and quality of experience (QoE) requirements of sea-going users. In the proposed ISI/ANR CE technique, we consider the effects of possible ISI that may arise from maritime transmissions in such a way that transformation using a low-pass filter is incorporated for eliminating the effects of channel noise in addition to the overall mitigation of the reverberations of multipath propagation. For realising the proposed RER technique, we normalise the Manhattan distance of the channel impulse response (CIR) and introduce a variable leakage factor controlled log-sum penalty function whose responsibility is to provide stability to the developed RER technique over existing techniques in all considered fading scenarios. A reweighting attractor is then added to further shrink the CE which then gives this scheme a performance advantage over all analysed estimators. As such, the contributions of this paper are outlined as follows:

- An IoT-based framework is designed for improving the QoS requirements in application to maritime operations and management where off-shore navigating vessels are equipped with environmental sensing equipment in communication with a CH user equipment that transmits aggregated seawater sensor information via the marine channel to a shoreward located central BS.
- We propose two novel CE techniques for improving the performances of maritime communication systems named RER and ISI/ANR CE that both attempt to improve the performance of conventional schemes such as maximum likelihood (ML) based estimation and recursive least squares (RLS) techniques in order to reduce the CE error of the maritime communication network using combinational techniques that involve summing the instantaneous square error with a log-sum penalty which is subsequently realised by the normalisation of the Manhattan distance of the system CIR. Additionally, simple step by step procedures for deriving our considered marine estimators is elaborately documented for the benefits of intending readers.
- We evaluate and document the QoS performance in terms of system data-rate, outage probability and QoS-guaranteed probabilities for improved nautical user QoE over signal transmission in both heavy frequent and light infrequent shadowing conditions of oceanic signal propagation. It is also establish from this work that proper CE methods can be adopted for improving the QoS and QoE of pelagic network users, where the proposed RER technique demonstrated a performance advantage over other customary schemes.

The rest of this paper is structured as follows. An overview of related works in the maritime industry is presented in

section II while a system model description of our IoMT framework is described in section III. In section IV, a description of the considered CE for IoMT is described after which the QoS requirement analysis and evaluation for the described IoMT framework is given in section V. The results obtained from simulation are discussed in section VI while section VII succinctly presents a summary of our findings in addition to recommendations of possible research directions. This article is concluded in section VIII.

II. OVERVIEW OF RELATED WORKS FOR IoMT

A limited number of research works have attempted to design and analyse the performances of various communication techniques which are capable of enhancing the operation of maritime activities. The benefits of IoT technology can be exploited in a variety of industries ranging from consumer electronics, healthcare, agriculture, industrial automation, transportation, construction, and maritime operations, etc. In IoMT technology, sensors and actuators are embedded over maritime equipment in order to achieve several goals ranging from environmental monitoring, offshore explorations, disaster mitigation and management, and assisted navigation [5]–[10]. To guarantee the QoS and QoE requirements of marine users, many factors including the consideration of wide network coverage area in addition to deployment of cost-effective systems must be considered for the modelling and the enabling of oceanographic propagations since maritime networks require wider signal coverages in comparison to their terrestrial counterparts. As such, the QoS requirements of over-sea users are expected to be satisfied similarly to that of other terrestrial applications. At this point, it is important to note that satellite broadband communication systems such as the international maritime satellite (INMARSAT) and maritime very small aperture terminal (MVSAT) systems can provide remarkable wide-area network coverages for maritime operations based on their very high frequency communication capabilities. Nevertheless, these communication systems are not cost-effective for the ever-increasing needs of marine users since they require high implementation cost to launch satellites into orbits, which require stabilizers for on-board antennas. Besides, very high frequency (VHF) aided terrene networks do not have the capacity to effortlessly support high data rate services due to the limited bandwidth. Consequently, there is a need to consider adopting cost-efficient terrestrial communication technologies to support the QoS requirements of maritime operations.

Based on the above statements, it is noteworthy to mention that green wireless networks are utilized as alternative sources of energy in modern-day maritime communication systems. The use of the aforementioned technology can significantly reduce the cost of establishing and maintaining maritime wireless networks. Exploiting the merits of this technology, the energy sustainability and network throughput for green energy-powered wireless nautical networks are evaluated in [11], where a green energy buffer is modelled as a G/G/1 queueing [11] system in which two heuristic algorithms are developed for the optimization of network energy sustainability and throughput. The proposed algorithms show that high network throughput and energy sustainability can be achieved for green-powered wireless communications.

The works in [5] and [6] made appreciable progress in the improvement of maritime communication systems by analysing the network performances of novel distributed antenna selection schemes which improved coastal communications using Wi-Fi and cellular links for data transmission. The author in [6] adopts the Rayleigh fading channel distribution for modelling the communication channel over signal transmissions involving various vessel-embedded marine user equipment (MUE) and the CH of specified vessels while the communication of the aggregated CH sensor information through the coastline mounted directional antenna to the remotely located cellular BS is modelled using the Rician fading channel distribution. It is important to state that this Rician distributed channel is known to be more applicable to propagation scenarios having a dominant line of sight (LoS) path between the transmitter and receiver. Finally, the works in [12] also made significant research in the marine industry by documenting state-of-the-art technical characteristics of viable high-speed maritime wireless networks, where the benefits of the fourth generation (4G) long term evolution (LTE) technology is exploited for the enhancement of network data rates over relatively large coverage areas. In addition, a testbed for the proposed LTE-maritime system as discussed in [12] is implemented, where documented experimental results show that the proposed LTE-Maritime system could be adopted as a reliable vessel-to-shore data communication network. Nonetheless, these works do not consider a systematised CE technique for enhancing maritime communication as it is assumed that full CSI is perfectly known at the receiving end of the cellular costal-mounted BS which is not always the situation in practice. As a result, the proposed systems may not optimally enhance the marine network coverage area in addition to system throughput especially in conditions where the channel experiences frequent heavy shadowing. This is because the actual CSI of the system is not well considered since the receiver detection techniques cannot guarantee enhanced network performances. Based on the aforementioned, the need to develop efficient CE schemes in order to guarantee accurate decoding of transmitting packets over maritime communication networks is necessary considering the unstable environmental factors usually exhibited across marine habitats.

To ensure the QoS requirements of marine users in addition to rendering improved QoE of nautical network users, we consider designing and evaluating two efficient CE schemes that take into veritable consideration, the actual fading characteristics of the CSI. To achieve this endeavour, the conventional ML and the adaptive RLS CE scheme are modified to improve the network performances of our developed oceanographic framework (in terms of outage

TABLE 1. List of main notations.

Notation	Description
$(.)^*$	Conjugation operator
$\vec{R}_i$	Data rate of vessel i
f_d	Doppler frequency
$\|.\|$	Euclidean norm
$\mathbb{E}$	Expectation operator
$\|.\|_F$	Frobenius norm operator
$\vec{\delta}[\ddot{D}_i, i]$	Gain vector of the adaptive estimator
$(.)^H$	Hermitian transpose operator
$P_{out}(.)$	Outage probability
$\overline{E}_p$	Power of the CH-aggregated signal
P_E	Power of the multipath component
$P_{QoS}(.)$	QoS-grarantee probability
$y[\ddot{D}_i, i]$	Received signal at service cloud
$\hat{C}_{RER}[\ddot{D}_i, i]$	RER channel estimate
$\hat{\varepsilon}$	RER Leakage factor
$\ddot{\epsilon}$	RER stability constant
sgn(.)	Signum function
γ_i	SNR at reception
μ	Step size parameter
$g[\ddot{D}_i, i]$	Transmitting information signal
σ_w^2	Variance of complex white Gaussian noise
$M_{a,b}(.)$	Whittaker function
$w[\ddot{D}_i, i]$	Zero-mean complex white Gaussian noise

probability and average data rate) for the overall improvement of maritime user QoE.

III. SYSTEM MODEL DESCRIPTION OF PROPOSED MARITIME SYSTEM

The shore side of maritime environment as considered in our system is illustrated in Fig. 1, where marine vessels are designed to effectively exploit the innumerable benefits of IoT technology in such a way that various varieties of sensors/MUE are embedded on vessels for monitoring diverse environmental and control system conditions. This is achieved by sending sensor information from well-positioned CH through coastline mounted DAs to a remotely located control station for essential analysis and decision making procedures. A description of the clustering process of the MUE that can propagate through Rayleigh fading channel to an on-shore mounted BS is described in this session.

A. DESCRIPTION OF THE CLUSTERING PROCESS

It is earlier mentioned that efficient and reliable communication methods such as sensor-based IoT technologies can be deployed during maritime operations for minimizing the blameworthy effects of maritime congestions in order to avoid ship-dock delays and marine accidents so that the QoE of marine users can be improved. The installation and exploitation of sensor networks around maritime vessels and the surroundings will alleviate the possibility of sudden/frequent occurrences of maritime queue formations, congestions and accidents since the sensor information can be configured to give maritime users early signals so as to make informed and early decisions for prevention of disaster occurrences. Consequently, relevant information such as the position, size, arrival time, unloading and departure time of individual ship can be predicted and collected for transmission to the seashore-located control station for processing in order to guarantee safe marine operations. Taking these points into consideration, there is a need to design suitable models for the transmission of the aggregated sensor information to the control station for decision making. As previously stated, individual vessels contain MUE known as cluster members (CM), where a CH is located in the centre of the vessel for signal transmission through the DA to the control station. If the set of oversea user type of equipment (i.e. MUE) is represented as $\ddot{\boldsymbol{E}}_i = \{1, 2, 3, \ldots, \ddot{e}_i\}$ (where $\ddot{e}_i$ is the total number of MUE on vessel i), while the set of DAs serving vessel i is represented as $\ddot{\boldsymbol{D}}_i = \{1, 2, 3, \ldots, \ddot{d}\}$ (where $\ddot{d}$ is the total number of DAs serving vessel i), then the distribution of the maritime wireless sensor nodes can be modelled using a Poisson-based modified *Neyman-Scott* cluster process. This clustering process generally consists of a union of clusters having a parent point in addition to numerous offsprings, where the parent process is characterised by homogeneous and poison-distributed processes (with intensity λ_p) while the offspring processes (MUE) are independently dispersed (with intensity λ_o) around their parents [13]–[15]. Since the distribution of the sensors that make up the maritime network are spatially clustered, the Neyman-Scott clustering process would be a suitable model for formulating the wireless sensor distributions because it considers a Poisson-based union of clusters that form a mother (or parent) process (such as a CH in a wireless sensor networks) with offspring (or daughter sensors) randomly surrounding their parent clusters. The Neyman-Scott process is selected to model the distribution of the maritime wireless sensor nodes because it is a flexible clustering method whose theoretical properties are easy to derive and simulate than other clustering methods like the log Gaussian Cox process, the Bartlett-Lewis (B-L) models in addition to processes like Binomial point and Bernoulli lattice processes. It is also established in [14] and [16] that this process (Neyman-Scott) is suitable for modelling spatially aggregated points. Two special cases of the Neyman-Scott cluster processes are *Matérn* and *Thomas* cluster processes. The former cluster process can be deployed for delineating the operational activities of the sensor-based maritime environment if the sensors are uniformly distributed to form a ball of dimension d and radius R whose density function is represented as:

$$f_{U_M}(u) = \begin{cases} \frac{d.u^{d-1}}{R^d} & \|u\| \leq \mathrm{R} \\ 0 & \text{otherwise} \end{cases} \quad (1)$$

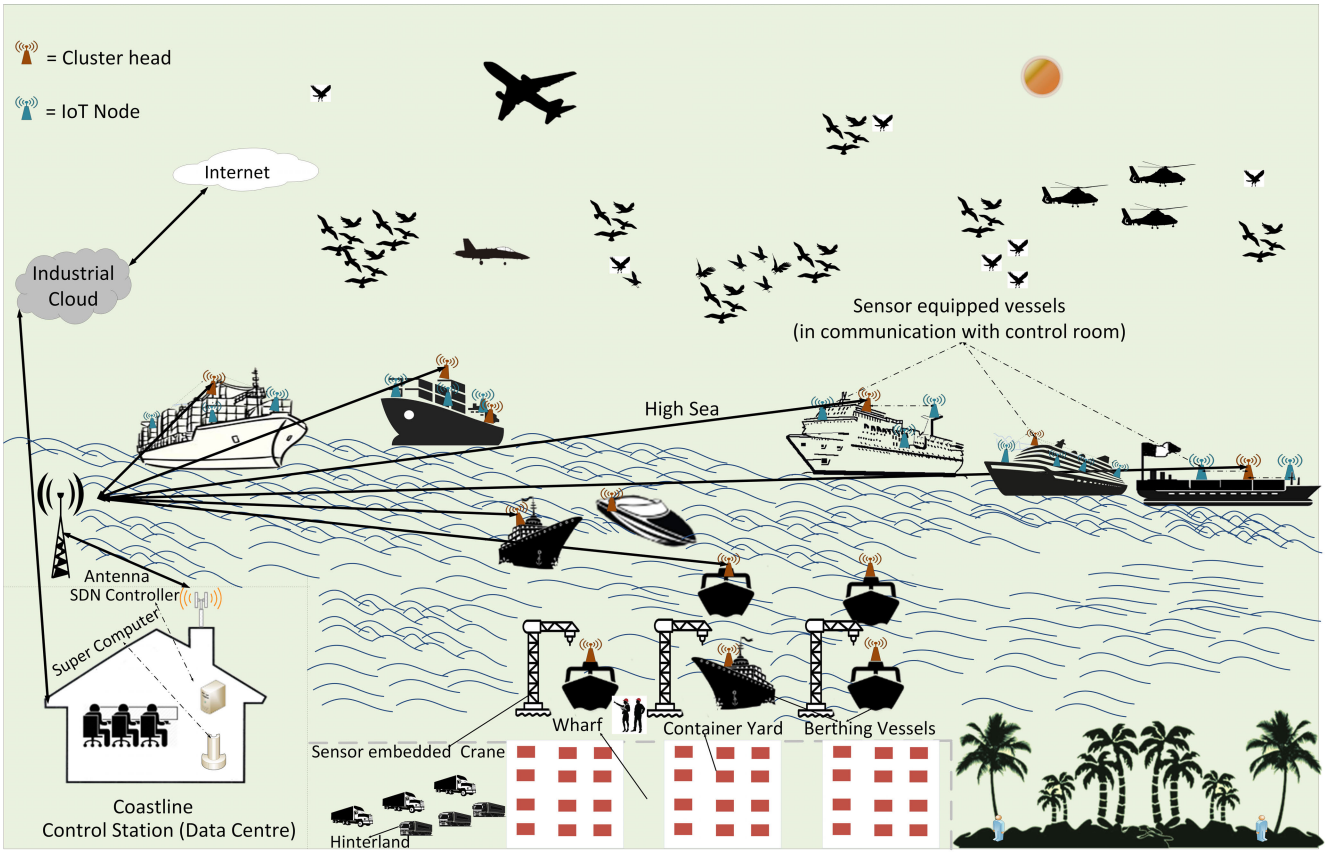

FIGURE 1. Framework structure of internet of things-based maritime environment.

where $\boldsymbol{u}$ in (1) represents the position (or location) of the MUE. On the other hand, if the clustering of the MUE is in accordance with a symmetric normal distribution (with variance σ^2), then the clustering process exhibits the characteristics of a Thomas cluster distribution. The Thomas cluster process is a more realistic distribution for simulating IoMT since the sensors are assumed to be scattered at various positions on individual vessels for environmental monitoring. Hence, if l_v and σ_n respectively represents the length of the vessel and the MUE clustering intensity, then the location of the MUE can be expressed using the Thomas cluster distribution as:

$$f_{U_T}(u) = (2\pi\sigma_n^2)^{-\frac{d}{2}} \exp\left(-\frac{1}{2\sigma_n^2}\|u\|^2\right) \quad \|u\|^2 \leq l_v \quad (2)$$

B. CHANNEL DESCRIPTION

It is worth mentioning that physical obstacles such as trees, buildings and mountains are limited across the open ocean which consequently enables a LoS path to be present across transmitter and receiver. Even if the effects of shadow fading on transmitting signals is minimal on oceanic wave propagations, the attenuation of propagating symbols across maritime environments can still be adversely affected by the effects of multipath-induced fading, particularly in situations of extreme weather conditions since the network performances can be influenced by factors such as rain, fog, oceanic waves and ship movements. As a result of this territorial variability, the Nakagami-*m* fading channel distribution will be most appropriate for modelling such environmental channel-fading scenarios since it offers remarkable flexibility attributes by altering two positive-valued parameters namely *shape factor* (m) and *spread controlling parameter* (Ω). In this Nakagami-based channel model, the shape factor (sometimes referred to as *fading parameter*) is adopted for varying the shape of the channel distribution in accordance with the gravity of the fading signal such that ($m \geq \frac{1}{2}$). On the other hand, the spread parameter is utilized for manipulating the delay spread, where ($\Omega \geq 0$). It is useful to note that the probability density function (PDF) of a Nakagami-*m* distribution is equal by definition to a Rayleigh fading distribution (where there is no LoS path) if $m = 1$. Whereas, this distribution will become a single-sided Gaussian distribution if $m \geq \frac{1}{2}$ and a uniform distribution in extreme scenarios when $m \to \infty$, thus confirming the flexibility of this channel model. Consequently, the Nakagami-*m* channel based on these parameters can be configured to enhance adaptive signal transmission over the communication channel in multipath fading environments. Nevertheless, we consider the Rayleigh fading scenario where $m = 1$ [17], [18]. It is assumed that the

coastline DAs are mounted thus stationary in position. Hence, the signal propagation can be modelled (in its worst-case scenario) as a Nakagami-m based single Rayleigh fading channel where the moment generating function (MGF) of $c[\ddot{D}_i, i]$ is generally expressed as:

$$M_h(s) = \frac{1}{\sqrt{\pi}\prod_{j=1}^{N}\Gamma(m_j)} \times G_{2,N}^{N,2}\left(\frac{4}{s^2}\prod_{j=1}^{N}\left(\frac{m_j}{\Omega_j}\right)\middle|\begin{matrix}0.5, 1\\ m_1, m_2, \ldots, m_N\end{matrix}\right) \quad (3)$$

In (3), $G(.)$ is the *Meijer's G-function* as described in [19] while m is the shape factor that usually assume values but not limited to the range $0.5 < m \leq 1$. Furthermore, Ω in (3) represents the *spread controlling* parameter while $\Gamma(.)$ is the *gamma function* as defined in [19]. Taking the inverse Laplace transform (ILT) of the expression in (3) (i.e. $L^{-1}(M_h(s))$, the PDF of $c[\ddot{D}_i, i]$ in accordance with the Nakagami-m distribution is given as [17], [18]:

$$f_G(g) = \frac{2}{\prod_{j=1}^{N}\Gamma(m_j)} G_{0,N}^{N,0}\left(g^2\prod_{j=1}^{N}\left(\frac{m_j}{\Omega_j}\right)\middle|\begin{matrix}-\\ m_1, m_2, \ldots, m_N\end{matrix}\right) \quad (4)$$

where g is the transmitted sensor information and the expression e^{-x} is generally given as $G_{0,1}^{1,0}\left(x\middle|\begin{matrix}-\\ 0\end{matrix}\right)$.

Two properties can be used to describe the characteristics of the Rayleigh fading channel. These properties are power spectral density (PSD) and the autocorrelation function (ACF). The PSD of the Rayleigh fading channel coefficients is given as [4]:

$$s|f| = \begin{cases} \frac{1}{\pi f_d\sqrt{1-\left(\frac{f}{f_d}\right)^2}} & |f| \leq f_d \\ 0 & otherwise \end{cases}$$

while the corresponding autocorrelation function is represented as:

$$a[\ddot{D}_i, i] = J_0(2\pi f_d T_s|\ddot{D}_i|) \quad (5)$$

Equation (5) represents the u-shaped band-limited Jakes spectrum. In this expression, f_d is the maximum Doppler frequency of the variable channel given as $f_d = \frac{v}{\lambda}$, where v is the velocity of the mobile CH while λ is the wavelength of the propagating symbols. Furthermore, $J_0(\cdot)$ is described as the zeroth-order Bessel function of the first kind while the symbol period and the normalized Doppler frequency (i.e. Doppler rate) is respectively given as T_s and $f_d T_s$. The correlation coefficients obtained from (6) can be used to form a correlation matrix $\boldsymbol{A_{cc}}$ whose expanded form as a function of the ACF is represented as:

$$A_{cc}[\ddot{D}_i] = \begin{bmatrix} a[1] & a[2] & \ldots & a[\ddot{d}] \\ a[2] & a[1] & \ldots & a[(\ddot{d}-1)] \\ \vdots & \vdots & \ddots & \vdots \\ a[\ddot{d}] & a[(\ddot{d}-1)] & \ldots & a[1] \end{bmatrix} \quad (6)$$

The channel fading coefficients can be realized using a complex recursive $\ddot{d}$th-order time-domain autoregressive (AR) process in the order of $AR(\ddot{d})$ given as:

$$c[\ddot{D}_i] = \sum_{i=1}^{\ddot{d}} z[i]c[\ddot{D}_i - i] + \vartheta[\ddot{D}_i] \quad (7)$$

where $\vartheta[\ddot{D}_i]$ is a zero mean additive white Gaussian noise process with variance given as σ_ϑ^2 while $z[i]$ is mathematically formulated as:

$$z[i] = -\boldsymbol{\varrho}[i] \quad (8)$$

If T represents the transpose operator, then the symbol $\boldsymbol{\varrho}[i]$ as used in (8) is define as:

$$\boldsymbol{\varrho}[i] = \left[\varrho[1], \varrho[2], \ldots, \varrho[\ddot{d}]\right]^T \quad (9)$$

besides, the variance of the noise process (σ_ϑ^2) can be represented as:

$$\sigma_\vartheta^2 = a[1] + \sum_{i=1}^{\ddot{d}} \boldsymbol{\varrho}[i]\boldsymbol{a}[i] \quad (10)$$

The coefficients of the AR model parameters $\vartheta[\ddot{D}_i]$ can be obtained using the Yule-walker equation [20] define as:

$$\boldsymbol{\varrho}[i] = -\boldsymbol{A_{cc}}^{-1}[i]\boldsymbol{b}[i] \quad (11)$$

where,

$$\boldsymbol{b}[i] = \left[a[1], a[2], \ldots, a[\ddot{d}]\right] \quad (12)$$

C. RECEIVER DESCRIPTION

It has been earlier mentioned that as marine vessels navigate across the high sea to the dock areas, the CHs in this IoMT system attempt to communicate with numerous seashore-mounted DAs as shown in Fig 2. A set of the coastal-mounted DAs configured to serve a particular vessel (or cluster) is known as a *service cloud* and the signals received at the cloud serving vessel i is given as:

$$y[\ddot{D}_i, i] = C[\ddot{D}_i, i]g[\ddot{D}_i, i] + w[\ddot{D}_i, i] \quad (13)$$

where $C[\ddot{D}_i, i]$ is a $\ddot{d} \times \ddot{d}$ diagonal matrix containing the channel coefficients that is obtained resulting from fading effects while $g[\ddot{D}_i, i]$ denotes the transmitted information signal vector that is received at the DAs. Lastly, $w[\ddot{D}_i, i]$ represents the zero mean complex white Gaussian noise with a variance σ_w^2 such that $w \sim \mathcal{N}(0, \sigma_w^2)$ while the received signal at service cloud i is given by $y[\ddot{D}_i, i]$ such that $y \sim \mathcal{N}(C\ g[\ddot{D}_i, i], \sigma_w^2)$. If the distance between the coastline-based DA a_k and vessel i is denoted as $z_{ak,i}$ while the path loss due to this distance from antenna is represented as $z_{ak,i}^{-\alpha}$, then the noise variance σ_w^2 is expressed as:

$$\sigma_w^2 = \frac{\overline{E}_p \sum_{k=1}^{\ddot{d}} \|C_{ak,i}\|^2 z_{ak,i}^{-\alpha}}{\gamma_i} \quad (14)$$

where the symbol α is regarded as the path loss exponent that takes value from 2 (free space propagation) to 6 (no LoS

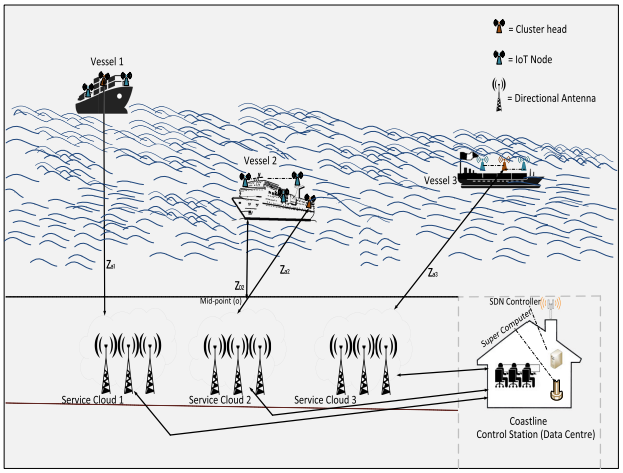

FIGURE 2. Illustration of cluster head communication with service clouds.

Propagation) [21]. In (14), $\overline{E}_p$ represents the power of the CH-aggregated signal given as $\mathbb{E}\left[g^2[\ddot{D}_i, i]\right]$, where $\mathbb{E}$ denotes the expectation operator and $\|.\|$ signifies Euclidean norm while γ_i is the SNR at the receiver side.

IV. CHANNEL ESTIMATION FOR MARITIME IoT

Since the propagation of transmitting signals across the marine environment can be perniciously affected by multipath-induced fading particularly in severe weather scenarios, the need for accurate estimation of the channel conditions is consequently necessary in order to guarantee excellent transmission and reception of propagating signals across the wireless maritime environment so as to make well-informed decisions. CE is thus, a worthwhile signal processing technique that is required at the receiver for combating the varying nature of the fading communication channel in order to ensure accurate detection of the propagating signals. At this point, it is important to remember that CE techniques can be broadly classified into three main categories including non-blind, semi-blind and blind CE. Non-blind CE can be further classified into two categories which are *training-based* (also referred to as pilot-assisted or data-aided) and *decision directed* estimation schemes. The pilot-based CE scheme adopts the use of receiver known training sequences named pilot signals for the estimation of the channel properties. Interested readers are referred to [4] for more information on the taxonomy of CE schemes.

In this paper, two channel estimators are proposed for estimating maritime transceivers which are based on improving the performances of conventional ML and RLS-based CE schemes for estimating the maritime fading channel conditions, where their performances are compared with conventional CE schemes such as normalised least mean squares (NLMS) and linear minimum mean square error (LMMSE) estimators. This is achieved by designing the estimators in such a manner that extra stability is given to enhance the quality of marine signals that are received over situations of both severe and non-severe environmental setups. The proposed estimation schemes are named ISI/ANR and RER channel estimators respectively. Table 2 gives an explicit summary of all considered estimators in a maritime context. In the following subsections, all estimators considered for implementation and comparison in our nautical communication framework are described elaborately.

A. NLMS CHANNEL ESTIMATION

To obtain improved CE performances based on the NLMS scheme, a cost function is deployed for minimizing the MSE of the maritime fading channel. This cost function is expressed as:

$$J_{cf}[\ddot{D}_i, i] = \mathbb{E}\left[|e_r[\ddot{D}_i, i, i]|^2\right] = \mathbb{E}\left[e_r[\ddot{D}_i, i]\, e_r^*[\ddot{D}_i, i]\right] \quad (15)$$

where $\mathbb{E}$ signifies the expectation operator and $*$ represents complex conjugation. In this expression (15), $e_r[\ddot{D}_i, i]$ denotes the CE error given in (16) where H represents the hermitian transpose operator, while $J_{cf}[\ddot{D}_i, i]$ signifies the cost function to be minimized.

$$e_r[\ddot{D}_i, i] = y[\ddot{D}_i, i] - C^H[\ddot{D}_i, i]g[\ddot{D}_i, i] \quad (16)$$

Furthermore, the term $C^H[\ddot{D}_i, i]g[\ddot{D}_i, i]$ is the inner product of the CH-aggregated sensor signal $g[\ddot{D}_i, i]$ and the corresponding LS estimate. Substituting the expression in (16) into (15), the cost function can then be written as the expression in (18), as shown at the bottom of the page, where the expression $e_r^*[\ddot{D}_i, i]$ as used in (15) is given as:

$$e_r^*[\ddot{D}_i, i] = y^*[\ddot{D}_i, i] - C[\ddot{D}_i, i]g^H[\ddot{D}_i, i] \quad (17)$$

To obtain the NLMS CE for the maritime communication, the LMS CE is first obtained after which it is then normalized using the power of the input signal according to (20). Hence, the LMS channel estimate of the marine communication network is given as:

$$\hat{C}_{LMS}[\ddot{D}_i + 1, i] = C[\ddot{D}_i, i] + \mu e_r^*[\ddot{D}_i, i]g^H[\ddot{D}_i, i] \quad (19)$$

where μ is defined as a fixed positive step size parameter that is responsible for controlling the steady-state behaviour of the adaptive CE scheme which is designed to satisfy the condition $0 < \mu < 1$. The derivation of the LMS CE scheme is shown in [22]. If the expression $\mu e_r^*[\ddot{D}_i, i]g^H[\ddot{D}_i, i]$ as given in (19) is normalized by the power of input signal $\left(||g^H[\ddot{D}_i, i]||^2\right)$ then the NLMS CE for the maritime communication system can be obtained as:

$$\hat{C}_{NLMS}[\ddot{D}_i + 1, i] = C[\ddot{D}_i, i] + \frac{\mu e_r^*[\ddot{D}_i, i]g^H[\ddot{D}_i, i]}{||g^H[\ddot{D}_i, i]||^2} \quad (20)$$

$$J_{cf}[\ddot{D}_i, i] = \mathbb{E}\left[(y[\ddot{D}_i, i] - C^H[\ddot{D}_i, i]g[\ddot{D}_i, i])(y^*[\ddot{D}_i, i] - C[\ddot{D}_i, i]g^H[\ddot{D}_i, i])\right] \quad (18)$$

TABLE 2. A summary of considered estimator characteristics for the internet of marine things.

Estimation Method	Algorithm Technique	Computational Complexity	Estimator performance
LS	Training-based	Low	Poor
LMMSE	Training-based	High	Low
ISI/ANR	Pilot-assisted	Medium	Good
NLMS	Pilot-assisted	Medium	Good
RLS	Data-aided	Very High	Very Good
RER	Data-aided	Highest	Best

B. PROPOSED ISI/ANR CHANNEL ESTIMATOR FOR MARITIME COMMUNICATION

The PDF of receiving a CH signal over the wireless fading channel is given as [23]:

$$f_Y(y[\ddot{D}_i, i]) = \frac{1}{\sqrt{2\pi\sigma_w^2}} \exp\left(-\frac{1}{2\sigma_w^2} \cdot \left(y[\ddot{D}_i, i] - C[\ddot{D}_i, i]g[\ddot{D}_i, i]\right)^2\right) \quad (21)$$

whereas, the joint PDF of the received signal vector (also referred to as the likelihood function of the channel estimate $\Lambda_L[y[\ddot{D}_i, i], C]$) is given as the product of the PDFs of the individual received signals which is represented as:

$$\Lambda_L[y[\ddot{D}_i, i], C] = \left(\frac{1}{\sqrt{2\pi\sigma_w^2}}\right)^{\ddot{d}} \exp\left(-\frac{1}{2\sigma_w^2} \cdot \sum_{\ddot{k}=1}^{\ddot{d}} \left(y[\ddot{k}] - C[\ddot{k}]g[\ddot{k}]\right)^2\right) \quad (22)$$

The natural logarithm of the above-expressed likelihood function is represented as:

$$\Lambda_{\log L}[y[\ddot{D}_i, i], C] = \ddot{d} \ln\left(\frac{1}{\sqrt{2\pi\sigma_w^2}}\right) - \left(\frac{1}{2\sigma_w^2} \cdot \sum_{\ddot{k}=1}^{\ddot{d}} \left(y[\ddot{k}] - C[\ddot{k}]g[\ddot{k}]\right)^2\right) \quad (23)$$

Thus, the maximum likelihood estimate of the fading channel is obtained by maximizing the log-likelihood function given as:

$$\hat{C}_{ML}[\ddot{D}_i, i] = \frac{\sum_{\ddot{k}=1}^{\ddot{d}} y[\ddot{k}]g[\ddot{k}]}{g^2[\ddot{k}]} \quad (24)$$

When the maritime communication channel experiences frequent heavy shadowing, there is a possibility that ISI may likely occur which is capable of degrading the reliability of maritime communication systems since propagating signals can face unpleasant distortions. To avoid spreading successive symbols beyond their assigned intervals, there is a need for CE procedures to re-consider the effects of possible ISI that may occur during transmission of sensor information in the maritime communication network. To minimize the effects of ISI in addition to channel noise during operation of coastal networks, the use of low-pass filtering can be incorporated for estimating the channel transfer function in order to significantly reduce the detrimental effects of these undesired phenomena. Inspired by the work in [24], we propose a novel CE technique that aims to improve the performances of conventional ML CE scheme, where the repercussions of the channel noise in addition to possible ISI that may result from multipath propagation are put into consideration. Our proposed improved ML-based CE scheme is named ISI/ANR channel estimation. Here, we reduce the upshot of noise by averaging the estimated channel parameters that are obtained from the ML estimation already established in (24). Consequently, the resulting ISI/ANR CE technique obtained by averaging the noise variance of the channel using the number of distributed antennas for augmenting the marine channel, provided that the expression in (13) is substituted into (24) is represented as in (25), shown at the bottom of the page.

Since the noise variance of the conventional ML-based channel estimate has been averaged to $\left[\ddot{d}^{-1}\sigma_w^2\right]$, the damaging consequences that can be potentially introduced by the noisy components of the maritime system are sequentially reduced. Taking the possibilities of signal distortions due to ISI into account, we further consider designing the maritime channel to meet the Nyquist ISI criterion by normalizing the combined ramifications of the channel noise and the ISI components using the Frobenius norm of the noise reduced ML-based channel estimate according to (25). As such, the noise-reduced transfer function of the maritime

$$\hat{C}_{ML_{AV}}[\ddot{D}_i, i] = g^{-2}[\ddot{k}]\left[\sum_{\ddot{k}=1}^{\ddot{d}}\left[\left(C[\ddot{D}_i, i]g[\ddot{D}_i, i] + \ddot{d}^{-1}w[\ddot{D}_i, i]\right)g[\ddot{k}]\right]\right] \quad (25)$$

$$\bar{\boldsymbol{\Upsilon}}_{RLS}^{-1}[\ddot{D}_i - 1, i] = \lambda^{-1}\bar{\boldsymbol{\Upsilon}}_{RLS}^{-1}[\ddot{D}_i - 1, i] - \lambda^{-1}\vec{\eth}[\ddot{D}_i, i]g^H[\ddot{D}_i - 1, i]\bar{\boldsymbol{\Upsilon}}_{RLS}^{-1}[\ddot{D}_i - 1, i] \quad (26)$$

channel is given as:

$$\hat{C}_{ANR}[\ddot{D}_i, i] = g^{-2}[\ddot{k}]\Bigg[\sum_{\ddot{k}=1}^{\ddot{d}}\Bigg[\Big(C[\ddot{D}_i, i]g[\ddot{D}_i, i] + \frac{1}{\|C_{ML}[\ddot{D}_i, i]\|_F}\Big(\vec{I}[\ddot{D}_i, i] + \ddot{d}^{-1}w[\ddot{D}_i, i]\Big)\Big)g[\ddot{k}]\Bigg]\Bigg] \quad (27)$$

where $\|.\|_F$ is the Frobenius norm operation while the expression $\left[\frac{1}{\|C_{ML}[\ddot{D}_i,i]\|_F}\left(\vec{I}[\ddot{D}_i, i] + \ddot{d}^{-1}w[\ddot{D}_i, i]\right)\right]$ consisting of the ISI component is a zero mean random Gaussian noise process. Because the channel conditions are known to change rapidly over time especially when the system experiences heavy shadowing/fading, the need to create system stability is inevitably required. As such, transformation using lowpass filtering is needed such that the modified ML-based channel transfer function for the maritime communication for noise reduction and ISI mitigation is written as:

$$\hat{C}_T[\ddot{\imath}] = \sum_{\ddot{k}=1}^{\ddot{d}} \hat{C}_{ANR}[\ddot{k}] \exp\left(-j\frac{2\pi}{\ddot{d}}\ddot{k}\ddot{\imath}\right) \quad (28)$$

where $\ddot{\imath}$ is the transformation index that takes values from $\ddot{\imath} \in [1, \ddot{d}]$ and reflects the variation speed of the frequency selective fading channel. To achieve lowpass filtering, the signals at high-frequency regions are zero-padded since the noise and ISI components are spread over this region while the vessel propagating sensor signal component is located at the lower frequency region.

C. DESCRIPTION OF THE PROPOSED RER CHANNEL ESTIMATION FOR MARITIME OPERATION

In this section, a description of our proposed RER CE algorithm is presented. To begin with, we review the conventional RLS CE where the cost function to be minimized for the channel estimate is given as [25]:

$$J_{cf}[\ddot{D}_i, i] = \sum_{i=1}^{\ddot{D}_i} \mathbb{F}[\ddot{D}_i, i]|e_r[\ddot{D}_i, i]|^2 \quad (29)$$

The symbol $\mathbb{F}[\ddot{D}_i, i]$ in (29) is the forgetting factor also known as weighting factor which assumes values in the range $0 \ll \mathbb{F}[\ddot{D}_i, i] < 1$. If λ is a positive constant chosen in the range $0 << \lambda < 1$, then the weighting factor can be expressed as:

$$\mathbb{F}[\ddot{D}_i, i] = \lambda^{D_i - 1} \quad (30)$$

If $\bar{\mathbf{\Upsilon}}_{RLS}[\ddot{D}_i, i]$ is expressed as the inverse autocorrelation matrix of the transmitting signal, then the gain vector of the RLS maritime channel estimate is given as:

$$\vec{\eth}[\ddot{D}_i, i] = \frac{\lambda^{-1}\bar{\mathbf{\Upsilon}}^{-1}_{RLS}[\ddot{D}_i - 1, i]g[\ddot{D}_i, i]}{1 + g^H[\ddot{D}_i, i]\lambda^{-1}\bar{\mathbf{\Upsilon}}^{-1}_{RLS}[\ddot{D}_i - 1, i]g[\ddot{D}_i, i]} \quad (31)$$

where $\bar{\mathbf{\Upsilon}}^{-1}_{RLS}[\ddot{D}_i - 1, i]$ is given as the expression in (26). Thus, the RLS channel estimate for the maritime communication system as derived in [22] is given as:

$$\hat{C}_{RLS}[\ddot{D}_i, i] = \hat{C}_{RLS}[\ddot{D}_i - 1, i] + \vec{\eth}[\ddot{D}_i, i]e^*_r[\ddot{D}_i, i] \quad (32)$$

Motivated by the concepts presented in [26], [27], we develop the proposed RER CE technique for our maritime communication system by formulating a new heuristic approach where the cost-function of the traditional RLS-based CE according to (29) is modified. In this modification, the aforementioned cost function is combined with a log-sum penalty presented as.

$$J_{cf_p}[\ddot{D}_i, i] = \sum_{i=1}^{\ddot{D}_i} \lambda^{D_i - 1}|e_r[\ddot{D}_i, i]|^2 + \hat{\varepsilon}\sum_{i=1}^{\ddot{D}_i} \log\left(1 + \ddot{\epsilon}^{-1}\left\|C[\ddot{D}_i, i]\right\|_1\right) \quad (33)$$

In the formulation of our RER heuristic, the Manhattan distance of the CIR is taken, which is subsequently normalised by a stability constant ($\ddot{\epsilon}$) whose responsibility is for correcting any potential numerical system instability that may arise during the updating stages of the CIR. In order to decrease the received signal error, the log-sum penalty function is eventually multiplied by an adjustable leakage factor $(\hat{\varepsilon})$ that provides additional stability to the oscillating channel behaviour in addition to minimizing the stalling of the channel coefficients under different marine fading conditions. This leakage factor takes value in the range $0 \leq \hat{\varepsilon} \ll 1$ and can be made adaptive using the variable leakage factor technique presented in [28] expressed as:

$$\hat{\varepsilon}[\ddot{D}_i + 1] = \hat{\varepsilon}[\ddot{D}_i] - \mu\Upsilon e^*_r[\ddot{D}_i, i]C[\ddot{D}_i, i]g^H[\ddot{D}_i, i] \quad (34)$$

where $\left[\Upsilon = \frac{\mu\hat{\varepsilon}}{\ddot{\epsilon}}\right]$. If $\epsilon = \ddot{\epsilon}^{-1}$, then the proposed RER channel estimate for maritime communication networks is given as:

$$\hat{C}_{RER}[\ddot{D}_i + 1, i] = C[\ddot{D}_i, i] - \Upsilon[\ddot{D}_i, i]\frac{\mathrm{sgn}C[\ddot{D}_i, i]}{1 + \epsilon C[\ddot{D}_i, i]} + \mu\vec{\eth}[\ddot{D}_i, i]e^*_r[\ddot{D}_i, i] \quad (35)$$

In (35), the expression $\left[-\Upsilon[\ddot{D}_i, i]\frac{\mathrm{sgn}C[\ddot{D}_i, i]}{1+\epsilon C[\ddot{D}_i, i]}\right]$ is a reweighting attractor that is adopted for shrinking (or reducing) the CE error. Additionally, the sgn function as used in this expression is the signum function which is defined as:

$$\mathrm{sgn}(\hat{C}) = \begin{cases} \frac{\hat{C}}{|\hat{C}|} & \text{if } \hat{C} \neq 0 \\ 0 & \text{if } \hat{C} = 0 \end{cases}$$

D. SEQUENTIAL PROCEDURES FOR IMPLEMENTING CE FOR IoMT

Simple simulation procedures for evaluating and analysing the system performances of the above-described maritime channel estimates assuming conventional and proposed methods are summarized as presented in Algorithm 1 and 2.

V. QoS REQUIREMENT ANALYSIS AND EVALUATION

The performance of the proposed maritime architecture according to Fig. 1 can be described and analysed for the CH-DA links in terms of data rate, outage probability and the QoS-guaranteed probability. The aforementioned performance indices are for our maritime communication system as follows:

A. AVERAGE DATA RATE REQUIREMENT FOR SHIP-DA LINK

Since the conditions of the wireless transmission channel of the marine environment fluctuates over time and can be adversely affected by multipath propagation and heavy shadowing, we model the average capacity of the IoMT network while exploiting the flexibility of the Nakagami-fading channel model in such a manner that situations of frequent heavy and infrequent light shadowing conditions are considered. As a result, the average data rate requirement of a ship navigating over Rayleigh fading conditions (where there is no LoS path between the aggregated CH signal and the BS-mounted DA) is analysed in addition to the Rician-fading scenarios where there is often a LoS component between DA-vessel transmission for maritime decision-making procedures as respectively presented in sections V-A1 and V-A2.

1) AVERAGE CAPACITY UNDER RAYLEIGH FADING CHANNEL

The maritime communication network is diagrammatically described in Fig. 2. In this figure, multiple offshore-positioned vessels are in communication with the seashore-mounted service cloud DAs. The achievable data rate (or capacity) of vessel i (denoted as $\vec{R}_i$) is mathematically given as [29]:

$$\vec{R}_i = \mathbb{E}_{C[\ddot{D}_i,i]}\left[\log_2\left(1+\gamma_i\right)\right] \tag{36}$$

where the SNR (γ_i) can be obtained from the expression in (14). As such, the expression in (36) becomes:

$$\vec{R}_i = \mathbb{E}_{C[\ddot{D}_i,i]}\left[\log_2\left(1+\frac{\overline{E}_p\sum_{k=1}^{\ddot{d}}\|C_{ak,i}\|^2 z_{ak,i}^{-\alpha}}{\sigma_w^2}\right)\right] \tag{37}$$

From (37), let $\hat{\tau}_h$ be represented as:

$$\hat{\tau}_h = \sum_{k=1}^{\ddot{d}}\|C_{ak,i}\|^2 z_{ak,i}^{-\alpha} \tag{38}$$

For simplicity, if $\zeta_k = z_{ak,i}^{-\alpha}$ then, the PDF of the generalized Erlang random variable according to the expression in (38) can be represented as:

$$\begin{aligned} f_{\hat{\tau}_h}(g) &= \sum_{k=1}^{\ddot{d}}\varpi_k(0) z_{ak,i}^{-\alpha}\exp(-z_{ak,i}^{-\alpha}g) \\ &= \sum_{k=1}^{\ddot{d}}\varpi_k(0)\zeta_k\exp(-\zeta_k g) \end{aligned} \tag{39}$$

Algorithm 1 Procedures for Realizing the Traditional Maritime Channel Estimation Schemes

Input: $\{g, c, \sigma_w^2, \gamma_{\text{dB}}, \ddot{\boldsymbol{d}}, \ddot{t}, \hat{\varepsilon}, \ddot{\epsilon}, \mu\}$
Output: $\{\boldsymbol{C_{ANR}}\}$

Generate random AWGN with zero mean and variance (σ_w^2) as given in (14), where γ_{dB} can be converted to linear scale using the expression $\left[\gamma_{\text{j}} = 10^{\frac{\gamma_{\text{dB}}}{10}}\right]$. Then compute the $\ddot{d} \times \ddot{d}$ diagonal matrix of CIR using the channel response obtained as described in section III-B.
From the generated Thomas cluster-based MUE and the simulated channel according to Algorithm 1 and 2 respectively, calculate the received signal at service clouds using (13).
for $j = 1$: Number of Iteration, **do**
  Evaluate the channel estimates as follows:
  for $E_b/N_o = 1$: length(γ_{j}) **do**
    % Evaluating LS channel estimate
    Compute diagonal matrix of transmit vectors given as $\left[G = diag(g, 0)\right]$
    Obtain the LS CE.
    Compute the MSE of the LS channel estimate.
    % Evaluating LMMSE channel estimate
    Compute sensor information matrix $\left[G = diag(g, 0)\right]$
    Evaluate cross and correlation Matrices given as $\boldsymbol{A_{cy}}$ and $\boldsymbol{A_{yy}}$ respectively.
    Generate the LMMSE maritime channel estimate.
    Compute the MSE of the LMMSE channel estimate.

    % Evaluating the NLMS channel estimate
    $\hat{C}_{NLMS} = zeros(1, \ddot{d})$ % Initializing NLMS channel estimate.
    for $i = 1$: Number of Iteration, **do**
      $\hat{C}_{NLMS}(1, 2{:}\text{end}) = \hat{C}_{NLMS}(1, 1{:}\text{end}-1)$. % Shifting frame coefficients of NLMS
      $\hat{C}_{NLMS}(1, 1) = \hat{C}_{LS}(i)$
      Choosing suitable step size parameter, evaluate the instantaneous error using (17) and compute the NLMS CE using (20).
      % Evaluating ISI/ANR channel estimate
      Create an empty cluster head product vector ($\boldsymbol{p_{CH}}$) in addition to empty transmitter-receiver vector signal ($\boldsymbol{p_{tr}}$).
    end for
  end for
end for
Return: {**c**}

where $\varpi_k(0)$ is the *Lagrange* basis polynomial in relation to ζ_k given as:

$$\varpi_k(0) = \prod_{\substack{0\le \dot{m}\le \ddot{d} \\ \dot{m}\neq k}} \frac{\zeta_{\dot{m}}}{\zeta_{\dot{m}} - \zeta_k} \tag{40}$$

Algorithm 2 Procedures for Realizing the Proposed Maritime Channel Estimators

schemes. **Input**: $\{g, c, \sigma_w^2, \gamma_{\text{dB}}, \ddot{\boldsymbol{d}}, \ddot{\imath}, \hat{\varepsilon}, \ddot{\epsilon}, \mu\}$

Output: $\{\boldsymbol{C_{ANR}}\}$

1: **for** $j = 1 : \ddot{d}$, **do**
2: $a_1 = y(j).g(j)$;
3: $a_2 = (g(j).^2)$;
4: $\boldsymbol{p_{tr}} = \left[\boldsymbol{p_{tr}}, a_1\right]$
5: $\boldsymbol{p_{CH}} = \left[\boldsymbol{p_{CH}}, a_2\right]$
6: **end for**
7: Compute the ML estimate of the marine channel using (24).
8: Minimize noise upshot by averaging the noise variance of the maritime channel using $\ddot{d}$ according to (27).
9: Enhance the channel stability by implementing the transformation expression given in (28).
10: % Evaluating the RER channel estimate
11: $\hat{C}_{RER} = zeros(1, \ddot{d})$
12: $\bar{\boldsymbol{\Upsilon}}_{RLS}(i, i) = inv(\lambda)$ % λ = regularization factor.
13: **for** $i = 1$: Number of Iteration, **do**
14: $\hat{C}_{RER}(1, 2{:}\text{end}) = \hat{C}_{RER}(1, 1{:}\text{end} - 1)$.
15: $\hat{C}_{RER}(1, 1) = \hat{C}_{LMMSE}(i)$
16: Compute the instantaneous error using (17).
17: Calculate inverse autocorrelation matrix using (26) and evaluate gain vector using (31).
18: To compare, compute the traditional RLS CE using (32).
19: Evaluate the variable leakage factor using (34).
20: Using the reweighting attractor expression, calculate the adaptive-based RER CE using (35).
21: **end for**

Return: {**c**}

Thus, the data rate of vessel i can be formulated as in (46).

2) AVERAGE CAPACITY ASSUMING SHADOWED-RICIAN FADING

The average data rate of vessel i over the maritime communication network assuming shadowed Rician fading is expressed as [5], [30]:

$$\vec{R}_i = \frac{1}{\ln 2}\int_0^{\infty} \ln\left(1 + \bar{\gamma} g\right) f_{\|C[\ddot{D}_i, i]\|^2}(g)\, \mathrm{d}g \tag{41}$$

where $\bar{\gamma}$ can be obtained from (14) as the ratio of the power of the CH-aggregated information to the noise variance. In the expression (41), the PDF $f_{\|C[\ddot{D}_i, i]\|^2}(g)$ can be obtained for shadowed Rician fading by taking the ILT of the MGF of $\|C[\ddot{D}_i, i]\|^2$, where the MGF of $\|C[\ddot{D}_i, i]\|^2$ is given as:

$$M_{\|C[\ddot{D}_i, i]\|^2}(s) = \frac{\eta(s+1)^{(1-\min[|\ddot{D}_i|, \varphi])}}{(2P_E)^{(2-\min[|\ddot{D}_i|, \varphi])}(s+\eta)^{m|\ddot{D}_i|}} \tag{42}$$

The notations m and Ω are as define in section III-B while η and φ are mathematically expressed as $\eta = \frac{m}{2mP_E + \Omega}$ and $\varphi = max[|\ddot{D}_i|, \lfloor m|\ddot{D}_i|\rfloor]$ respectively. Furthermore, the greatest of the two positive integers is chosen for the $max[.,.]$ operation while the smallest is chosen for the $min[.,.]$ operation. Finally, the symbol $\lfloor . \rfloor$ is the floor operation which represents the largest integer not greater than the expression (.) while $2P_E$ is the average power of the multipath component. Taking the ILT of (42), the PDF of the SNR (γ_i) given that $(\gamma_i) > 0$ is expressed as:

$$f_{\gamma_i}(g) = \sum_{\hat{l}=0}^{\xi} \binom{\xi}{\hat{l}} .(2P_E)^{((m-1)|\ddot{D}_i|)} \Big(\mathcal{F}(g, \hat{l}, \varphi, \bar{\gamma}_i) + \eta\phi\mathcal{F}(g, \hat{l}, \varphi + 1, \bar{\gamma}_i)\Big) dg \tag{43}$$

where $\xi = \left(\varphi - |\ddot{D}_i|\right)^+$ and $(g)^+$ shows that if $g \leq 0$ then use $g = 0$. In addition, the function $\mathcal{F}(g, \hat{l}, \varphi, \bar{\gamma}_i) = \frac{\eta^{(m|\ddot{D}_i| - \varphi)}}{\bar{\gamma}_i^{\frac{1}{2}(\varphi - \hat{l})}\Gamma(\varphi - \hat{l})} . g^{\frac{1}{2}(\varphi - \hat{l}) - 1} \exp(-\frac{\eta}{2\bar{\gamma}} g) \left[M_{\frac{1}{2}(\eta + \hat{l}), \frac{1}{2}(\varphi - \hat{l} - 1)}\left(\frac{\eta}{\bar{\gamma} g}\right)\right]$, while $M_{a,b}(.)$ is the Whittaker function bearing in mind that the symbol ϕ in (43) is given as $\phi = \frac{\omega(m|\ddot{D}_i| - \varphi)}{2mP_E}$. Converting the expression in (43) to its Kummer's function equivalent and simplifying further gives the average data rate expression (assuming shadowed Rican fading) as presented in (44), shown at the bottom of the next page.

B. QoS REQUIREMENT EVALUATION FOR SHIP-DA LINK

1) OUTAGE PROBABILITY FOR CH-DA COMMUNICATION

A certain minimum signal level (or threshold) is required for acceptable performance of maritime communication networks. If excellent communication techniques are not well developed for the maritime communication systems, then the CH-DA transmission processes may experience outages that may result from the devastating effects of environmental fading conditions. Outage probability (P_{out}) is a useful metric (or parameter) that is required for the characterisation of network performances in communication systems and can simply be described as the probability that the received information rate falls below a certain required threshold, which further describes the probability that a system outage will take place over a specified period. For the described maritime communication system, the outage probability of the vessel-DA transmission is symbolically defined as $\left[P_{out}(\gamma_i) \triangleq P_{out}(\gamma_i \leq \gamma_i^{th}) = P_{out}(\vec{R}_i \leq \vec{R}_i^{th}) = F_{\vec{R}_i}(\vec{R}_i^{th})\right]$,where $Pr(.)$ denotes probability and $F_{\vec{R}_i}(.)$ represents the cumulative density function (CDF) such that $\left[F_{\vec{R}_i}(g) = \int_0^g f_{\vec{R}_i}(g)\, dg\right]$ and $f_{\vec{R}_i}(.)$ is the PDF as previously described.

It can be observed from (37) that the data rate for the clustered maritime communication system assuming Rayleigh fading scenarios is given as $\vec{R}_i = \left[\log_2\left(1 + \frac{\overline{E}_p \hat{\tau}_h}{\sigma_w^2}\right)\right]$. From this expression, if $\hat{\tau}_h$ is expressed in terms of the data rate, then the outage probability of the vessel- DA link can easily be computed bearing in mind that $P_{out}(\gamma_i) = F_{\hat{\tau}_h}(\hat{\tau}_h)$. Thus, after simple mathematical analysis, it can easily be deduced that $\left[\hat{\tau}_h = \frac{\sigma_w^2}{\overline{E}_p}\left(e^{\vec{R}_i \log_e 2} - 1\right)\right]$. Consequently,

the outage probability of the maritime system under non-LoS (NLOS) propagations can be simply be expressed as:

$$P_{out}\left(\vec{R}_i^{th}\right) = F_{\hat{\tau}_h}\left(\hat{\tau}_h\right) = F_{\hat{\tau}_h}\left(\frac{\sigma_w^2}{\overline{E}_p}\left(e^{\vec{R}_i \log_e 2} - 1\right)\right) \quad (47)$$

Solving the expression in (47) yields the Rayleigh fading outage probability expression given in (45). Since the CDF of the outage probability is expressed as $F_{\vec{R}_i}(g) = \int_0^g f_{\vec{R}_i}(g)\, dg$ and the data rate requirement of the ith vessel according to (36) is generally related to the SNR as $\vec{R}_i = \left[\log_2\left(1+\gamma_i\right)\right]$, then the outage probability assuming Rician fading channel can be obtained if γ_i (in the above data rate expression) is made the subject of the relation. Hence,

$$\begin{aligned} P_{out}\left(\vec{R}_i^{th}\right) &= F_{\gamma_i}(\exp(\log_e 2.\vec{R}_i^{th}) - 1) \\ &= \sum_{\hat{l}=0}^{\xi} \binom{\xi}{\hat{l}} .(2P_E)^{((m-1)|\ddot{D}_i|)} \Big(\mathcal{G}(g, \hat{l}, \varphi, \bar{\gamma}_i) \\ &\quad + \eta\phi\mathcal{G}(g, \hat{l}, \varphi+1, \bar{\gamma}_i)\Big) dg \end{aligned} \quad (48)$$

where $g = (e^{(\log_e 2.\vec{R}_i^{th})} - 1)$ while from the expression shown in (48), $\mathcal{G}(g, \hat{l}, \varphi, \bar{\gamma}_i)$ is given as:

$$\begin{aligned} &\mathcal{G}(g, \hat{l}, \varphi, \bar{\gamma}_i) = \int_0^g \mathcal{F}(g, \hat{l}, \varphi, \bar{\gamma}_i) \\ &= \int_0^g \mathcal{F}(g, \hat{l}, \varphi, \bar{\gamma}_i) = \left[\frac{\eta^{(m|\ddot{D}_i|-\varphi)}}{\bar{\gamma}_i^{\frac{1}{2}(\varphi-\hat{l})}\Gamma(\varphi-\hat{l})}\right. \\ &\left. .\left(e^{\left(\log_e 2.\vec{R}_i^{th}\right)} - 1\right)^{\frac{1}{2}(\varphi-\hat{l})-1} .\exp\left(-\frac{\eta}{2\bar{\gamma}}.\left(e^{\left(\log_e 2.\vec{R}_i^{th}\right)}\right.\right.\right. \\ &\left.\left.\left. - 1\right)\right)\right] \times \left[M_{\frac{1}{2}(\eta+\hat{l}),\frac{1}{2}(\varphi-\hat{l}-1)}\left(\frac{1}{\bar{\gamma}}\right).\left(\frac{\eta}{(e^{(\log_e 2.\vec{R}_i^{th})} - 1)}\right)\right] \end{aligned} \quad (49)$$

The equation in (48) is thus, the outage probability expression of ship i in relation to the rate threshold $\vec{R}_i^{th}$.

2) QoS-GUARANTEED PROBABILITY EVALUATION

The QoS-guaranteed probability for a marine vessel i is the probability requirement that satisfactory services are provided by the communication network of vessel i. This service probability can be generally expressed for both frequent heavy shadowing and infrequent light shadowing conditions. When the transmission channel experiences Rayleigh fading, the QoS-guaranteed probability is given as [6]:

$$\begin{aligned} P_{QoS}\left(\vec{R}_i^{th}\right) &= Pr\left\{\vec{R}_i \geq \vec{R}_i^{th}\right\} \\ &= Pr\left\{\log_2\left(1 + \frac{\overline{E}_p\hat{\tau}_h}{\sigma_w^2}\right) \geq \vec{R}_i^{th}\right\} \\ &= 1 - F_{\hat{\tau}_h}\left(\hat{\tau}_h\right) = 1 - F_{\hat{\tau}_h}\left(\frac{\sigma_w^2}{\overline{E}_p}\left(e^{\vec{R}_i \log_e 2} - 1\right)\right) \end{aligned} \quad (50)$$

On the other hand, the QoS requirement assuming infrequent light shadowing is given as:

$$\begin{aligned} P_{QoS}\left(\vec{R}_i^{th}\right) &= Pr\left\{\vec{R}_i \geq \vec{R}_i^{th}\right\} \\ &= Pr\left\{\log_2\left(1+\gamma_i\right) \geq \vec{R}_i^{th}\right\} \\ &= 1 - F_{\gamma_i}\left(\gamma_i\right) = 1 - F_{\gamma_i}\left(e^{\vec{R}_i \log_e 2} - 1\right) \end{aligned} \quad (51)$$

C. SEQUENTIAL PROCEDURES FOR PERFORMANCE EVALUATION AND COMPARISON

Simple simulation procedures for evaluating and analysing the system performances of the above-described maritime system in terms of QoS requirements are summarized as presented in Algorithm 3.

$$\begin{aligned} \vec{R}_i = \frac{1}{\ln 2}(2P_E)^{((m-1)|\ddot{D}_i|)}.\eta^{(m|\ddot{D}_i|-\varphi)} \sum_{\hat{l}=0}^{\xi} \\ .\left[\left(\frac{\eta^{-(\varphi-\hat{l})}}{\Gamma(\varphi)}\right) G_{4,3}^{2,3}\left(\frac{-\bar{\gamma}}{\eta}\middle| \begin{matrix} -\varphi+\hat{l}+1, 1, 1, 0 \\ \hat{l}, 1, 0 \end{matrix}\right) + \left(\frac{\phi.\eta^{\varphi-\hat{l}-1}}{\Gamma(\varphi+1)}\right).G_{4,3}^{2,3}\left(\frac{-\bar{\gamma}}{\eta}\middle| \begin{matrix} -\varphi+\hat{l}, 1, 1, 0 \\ \hat{l}, 1, 0 \end{matrix}\right)\right] \end{aligned} \quad (44)$$

$$\begin{aligned} P_{out}\left(\vec{R}_i^{th}\right) = \frac{1}{\log_e(2)} \sum_{k=1}^{\ddot{d}} \varpi_k(0) \\ \times\left[-\left(e^{-\zeta_k\left(\frac{\sigma_w^2}{\overline{E}_p}\left(e^{\vec{R}_i \log_e 2}-1\right)\right)}.\log_e\left(1 + \frac{\overline{E}_p\left(e^{\vec{R}_i \log_e 2} - 1\right)}{\sigma_w^2}\right) + \left(e^{\frac{\zeta_k\sigma_w^2}{\overline{E}_p}} E_1\left(\zeta_k\left(e^{\vec{R}_i \log_e 2} - 1\right) + \frac{\zeta_k\sigma_w^2}{\overline{E}_p}\right)\right)\right)\right] \end{aligned} \quad (45)$$

$$\vec{R}_i = -\frac{1}{\log_e(2)} \sum_{k=1}^{\ddot{d}} \varpi_k(0)\left[\left(e^{-\zeta_k g}\log_e\left(1 + \frac{\overline{E}_p g}{\sigma_w^2}\right)\right) + \left(e^{\frac{\zeta_k\sigma_w^2}{\overline{E}_p}} E_1\left(\zeta_k g + \frac{\zeta_k\sigma_w^2}{\overline{E}_p}\right)\right)\right] \quad (46)$$

VI. SIMULATIONS AND DISCUSSIONS OF RESULTS

In order to analyse and validate our proposed methods, we present comparative graphical results where the performances of RER and ISI/ANR CE schemes are evaluated in terms of mean square error (MSE) at various levels of SNR. Furthermore, we also evaluate the performances of the maritime network using average data rate and outage probability as a metric. In these simulations, the MUEs are assumed to be embedded at random positions on the individual marine vessels in such a way that their distribution can be modelled by the well-known Thomas cluster processes. To prepare the

Algorithm 3 Procedures for Network Performance Evaluation and Analysis

Input: $\{g, \zeta_k, m, P_E\}$
Output: $\{\vec{R}_{\text{Ray}}, \vec{R}_{\text{Rice}}, P_{NLoS}, P_{LoS}\}$

1: **for** $i = 1$: Number of Iteration, **do**
2: **for** $E_b/N_o = 1$: length(γ_j) **do**
3: Compute the path loss based Lagrange basis polynomial $\left(\varpi_k(0)\right)$ using (40).
4: Evaluate the power of aggregated CH-signal $\left(\mathbb{E}\left[g^2[\ddot{D}_i, i]\right]\right)$.
5: Calculate the data rate $\left(\vec{R}_{\text{Ray}}\right)$ over Rayleigh fading scenario using (46).
6: Evaluate the data rate $\left(\vec{R}_{\text{Rice}}\right)$ over Rician fading scenario using (44), considering the parameter definitions described in section V-A2.
7: Compute the outage probability $\left(P_{NLoS}\right)$ over NLoS propagtion using (45).
8: Evaluate the outage probability $\left(P_{LoS}\right)$ over infrequent light shadowing based on (48).
9: **end for**
10: **end for**

Return: $\{\vec{R}_{\text{Ray}}, \vec{R}_{\text{Rice}}, P_{NLoS}, P_{LoS}\}$

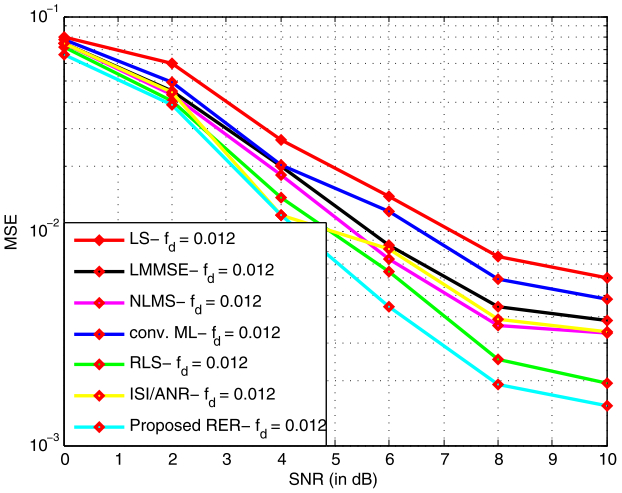

FIGURE 3. Mean square error performance of estimators versus signal to noise ratio given $f_d T_s = 0.0119$.

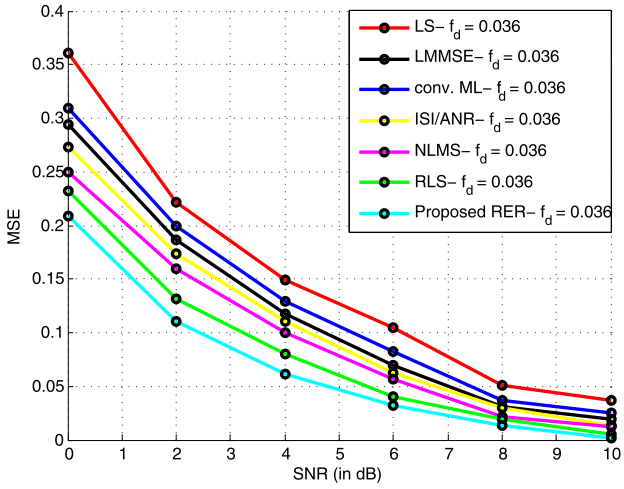

FIGURE 4. Mean square error performance of estimators versus signal to noise ratio given $f_d T_s = 0.0358$.

maritime communication system for resilience in times of adversities such as multipath-induced fading, the Nakagami-m fading model is considered for the marine model in order to checkmate the effects of frequent heavy, average and infrequent light showing conditions over the maritime environment. In the period when the oceanic surroundings battle the effects of burdensome shadowing, the Rayleigh fading channel model is best applicable (in worst-case scenarios) for evaluating the signal propagation performances where the fading parameter of the Nakagami-m channel equals unity. On the contrary, the Rician channel model is applicable under LOS CH transmissions whose average data rate requirements have been elaborately described in section V-A2.

Marine vessels are conventionally assigned speed limits as they sail through the ocean. Various intercontinental seaports assign specific speed limits across seawater harbours which substantially depends on the kind of ship deployed. The allocated average speed limit ranges from 10 (18.52 km/hr) - 30 (55.56 km/hr) knots. It is worthy to remember that the channel transfer function is more likely to experience slow fading when ships travel at the lower speed limits. Conversely, coastal communication systems will experience fast fading channel behaviours when marine vessels propagate their signals at the upper-speed limit. If the Doppler frequencies corresponding to slow and fast fading maritime channels is chosen as 10 Hz and 36 Hz respectively, then complementary wavelength for the afore-mentioned channel conditions will be 0.431 m. More so, if the Doppler frequencies are normalized by a sampling period (T_s) of 10^{-3} s, then the normalized Doppler frequencies corresponding to slow and fast maritime channel fading with bandwidth of 1000 Hz will correlate to 0.0119 and 0.0358 respectively.

Figures 3 - 9 show graphical illustrations of the CE performances of our proposed algorithms in comparison to other customary CE techniques as can be deployed in the operation of maritime communication networks. The performances of the estimators are analysed through Monte-Carlo simulations with 100,000 trials per SNR. First, we evaluate and compare

TABLE 3. Simulation parameters.

Parameter	Specification
Step-size Parameter	0.50
RER Stability Constant	0.1
Cluster Intensity	0.3
Path Loss Exponent	2.4 (LoS), 4.68 (NLoS)
Average Power	1.29 (LoS), 8.97×10^4 (NLoS)
Shape Factor	19.4 (LoS), 1 (NLoS)
Doppler Rates	0.012 (Slow Fade), 0.036 (Fast Fade)
Channel Type	Rayleigh/Rician Fading

our proposed CE schemes with existing techniques given that the communication between offshore navigating vessels and the seashore positioned BS occurs under slow fading and fast fading conditions respectively. As shown in Fig. 3 and 4, the performances of the proposed ISI/ANR estimator significantly improves the characteristics of conventional ML estimator. This is due to the fact that this estimator, in particular, considers the effects of marine channel noise in addition to possible effects of ISI that could arise during signal transmissions. Here, the noise variance of the nautical channel is averaged in order to reduce the possibility of noise upshoot, where the Frobenius norm of the estimated CSI obtained from ML technique is used to normalise possible ISI component of the propagating maritime signal. The resulting channel estimate is then transformed using lowpass filtering in order to further suppress unwanted channel noises and interferences. More so, simulation results further demonstrate that improved system CE can be achieved for the operation of nautical networks using the ISI/ANR estimator in comparison with other linear estimators such as the orthodox least squares (LS) and linear minimum mean square error (LMMSE) CE schemes due to the aforementioned reasons. It is further observed from Fig. 3 and 4 that the proposed RER CE method offers superior MSE performances in comparison to the conventional RLS in addition to the proposed ISI/ANR CE schemes. This is because the RER technique introduces system stability by the Manhattan distance normalisation of the CIR using a stability constant during the updating phase of the CIR. Moreover, the addition of a re-weighting attractor is adopted for providing additional network stability which offers the proposed adaptive RER technique the advantage to converge faster in comparison to other considered adaptive schemes including the customary RLS technique and the static step-size based NLMS method (as shown in Fig. 5) at an SNR of 10 dB. To be more specific, at an MSE of 10^{-2}, the RER method under slow fading channel shows a performance gain of about 1 dB when compared to the traditional RLS method while similarly showing superiority gain of about 0.6 dB over RLS method assuming fast fading channel conditions as depicted in Fig. 4. For IoMT applications, the adaptive NLMS CE scheme positive step size parameter is chosen as 0.50 in order to provide an intermediate concession between nautical signal propagations assuming heavy frequent marine channel shadowing

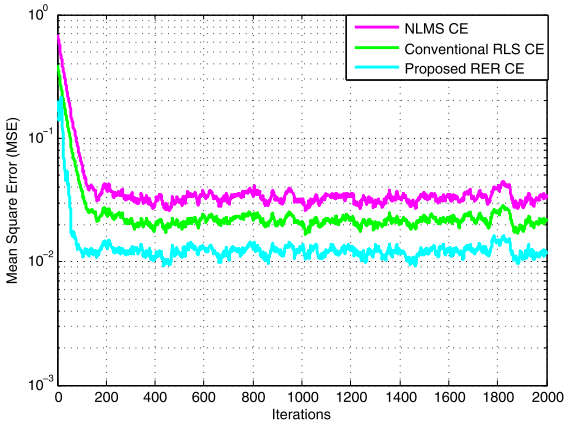

FIGURE 5. Convergence behaviour of proposed RER channel estimator in comparison to RLS and NLMS under slow fading conditions.

scenarios and LOS signal transmissions. In other words, appreciable system stability is offered using this value. More so, this research shows that the estimation scheme becomes unstable outside the optimal range of $0.40 \leq \mu \leq 0.50$ since the formidable convergence and steady-state behaviour of the algorithm cannot be easily administered outside this region. Furthermore, it is demonstrated that choosing a higher value of μ within this optimal range will guarantee better system stability for the adaptive NLMS and RER algorithms as shown in Fig. 6.

For the proposed adaptive RER CE technique, a forgetting factor of 0.998 is used because it is shown in [25] that this value yields good results for customary RLS estimators. Additionally, a regularization factor of 0.001 is used for initializing the inverse autocorrelation matrix of the RER estimate according to (26) while it is shown from this research that this algorithm achieves optimal stability when the stability constant offers extra sturdiness to the variable leakage factor in the range of $0.06 \leq (\ddot{\epsilon}) \leq 0.1$. Hence, a better MSE is obtained as $(\ddot{\epsilon})$ increases within the stability region under both heavy frequent shadowing propagation and steady fading channel scenarios as depicted in Fig. 7 and 8 respectively. It can also be generally observed that the maximum constant within the stability region yields superlative CE for the maritime signal transmissions while constants with magnitude above this region impacts negatively on the steady-state behaviour of this estimation algorithm. More so, the higher the Doppler spread, the poorer the estimation performance as delineated in Fig. 9 where the adaptive estimation performances are analysed for different values of Doppler spread at an SNR of 5 dB. In other words, the CE performances are directly proportional to the magnitude of the normalized Doppler frequency.

The performances of the described nautical network architecture according to Fig. 1 are then evaluated in terms of average data rate and QoS requirements for the offshore navigating vessel to sea-shore mounted DA communications, where it is established that the use of CE can significantly improve the QoS and QoE of thalassic networks. The data

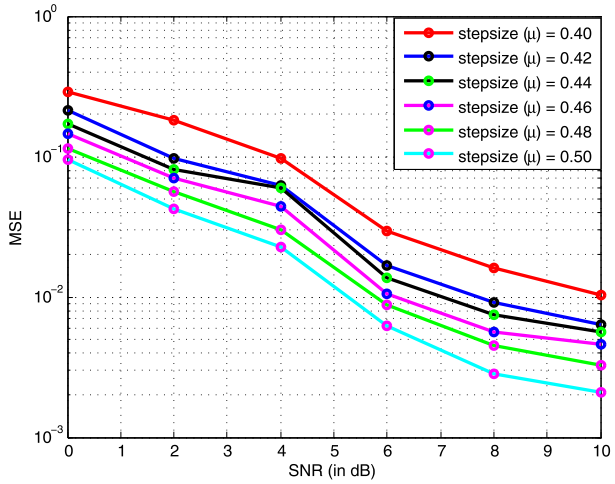

FIGURE 6. A comparison of mean square error versus signal to noise ratio at different step size for proposed adaptive RER and NLMS channel estimation schemes.

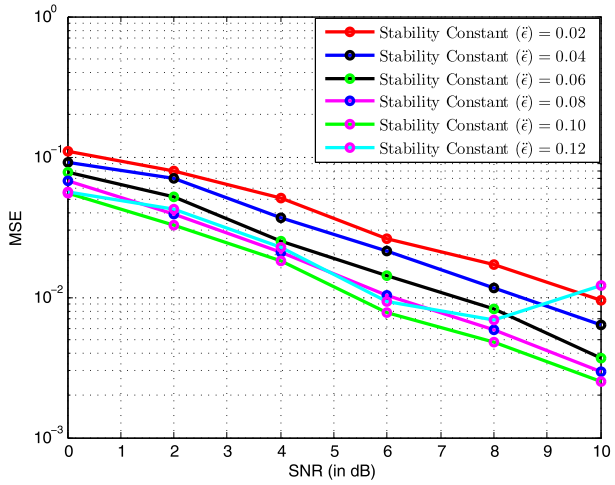

FIGURE 7. Comparative analysis of CE MSE versus SNR at different stability constants for proposed adaptive RER assuming slow fading NLoS propagations.

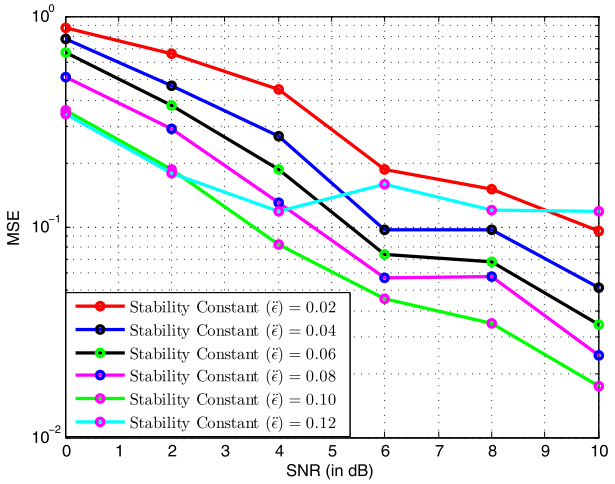

FIGURE 8. Comparative analysis of mean square error versus signal to noise ratio at different stability constants for proposed RER assuming fast fading NLoS propagations.

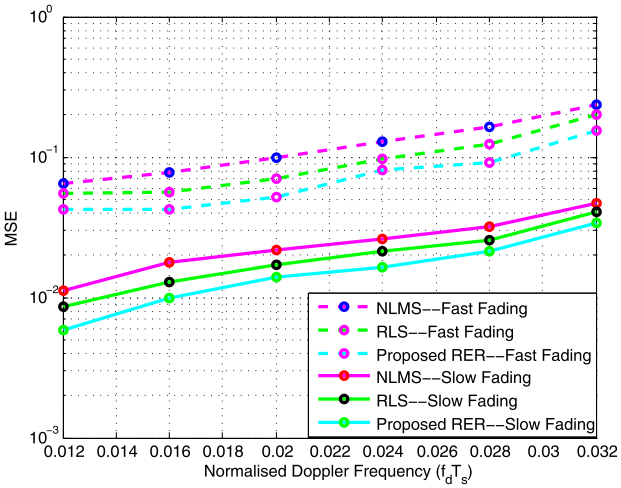

FIGURE 9. A comparative illustration of mean square error versus Normalised Doppler frequency at SNR = 5 dB for adaptive estimators assuming slow and fast fading.

rate requirements of the maritime communications are principally evaluated assuming LoS and NLoS propagations (which correspond to a Nakagami shape factor of $m = 19.4$ [30] and $m = 1$ respectively). More so, the average power (Ω) of both the LoS and NLoS communication, corresponds to 1.29 and 8.97×10^{-4} respectively [30]. On the other side, the outage probability and QoS guaranteed probability is evaluated for both frequent heavy and infrequent light shadowing conditions of CH-DA communications. The simulated and theoretical results illustrated in Fig. 10 and 11 show that the average data rate increases as the SNR of transmission increases and vice-versa. Also, the marine network will offer a higher data rate over Rician fading channel scenarios in comparison to Rayleigh fading propagations. We can also deduce from these figures that as the number of DAs is increased in the service cloud, the average system data rate increases directly. For example, it is noted from Fig. 10 that as the SNR value rises from 4 dB to 8 dB under Rician fading conditions, there is a significant increase in the data rate output. To be more specific, it is observed that when 5 DAs are employed for the marine communication network per service cloud, the data rate increases from a just a little over 75 bps to about 82 bps when SNR values change from 4 dB to 8 dB respectively. A similar trend is also achieved under the Rayleigh fading channel propagation scenario. More so, it is deciphered from Fig. 11 that as the number of DA increases in the coastal communication network, the system data rate increases proportionally. The data rate characteristics are further analysed and expanded as represented in Fig.12 for SNR values ranging from 4 to 10 dB over both LoS and NLoS communication systems. It can be seen from the bar graph that the data rate improves when there is a LoS path along the marine communication network in comparison to when there is no LoS propagation. Another visible observation from this chart shows that increasing the number of DA over the maritime communication system will consequently result

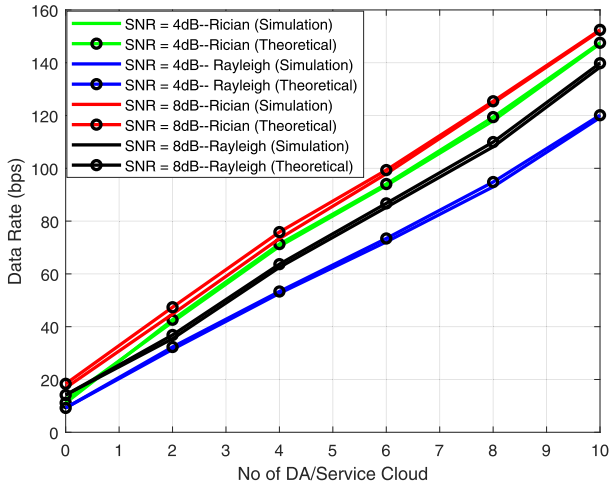

FIGURE 10. A juxtaposition of average data rate vs number of directional antenna per service cloud over Rician and Rayleigh fading for signal to noise ratios of 4 and 8 dB.

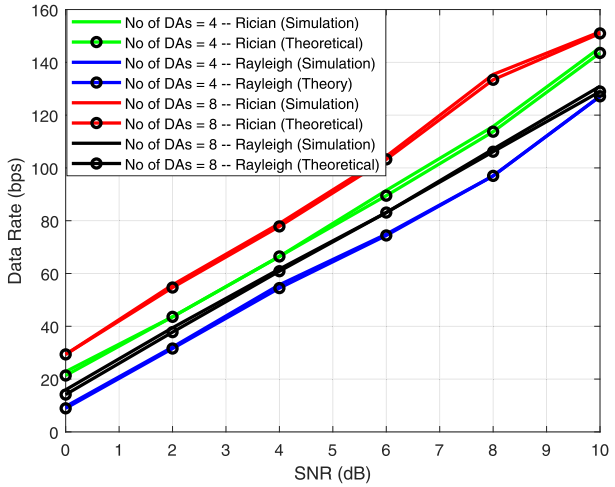

FIGURE 11. A juxtaposition of average maritime data rate vs signal to noise ratio over Rician and Rayleigh propagation for 4 and 8 directional antenna per service cloud.

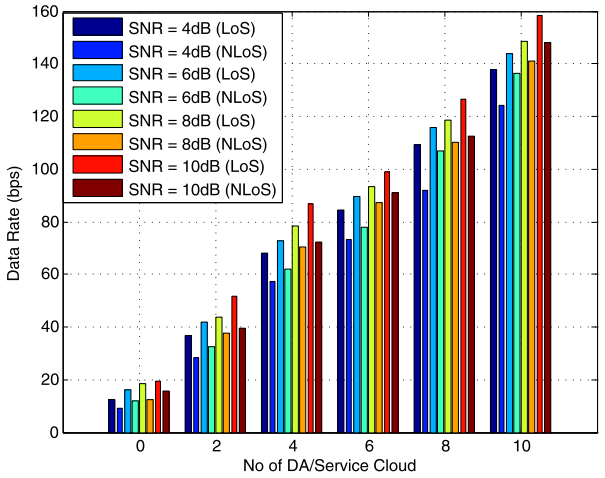

FIGURE 12. A plot of average data rate vs number of directional antenna per service cloud over LoS and NLoS propagation at different signal to noise ratio values.

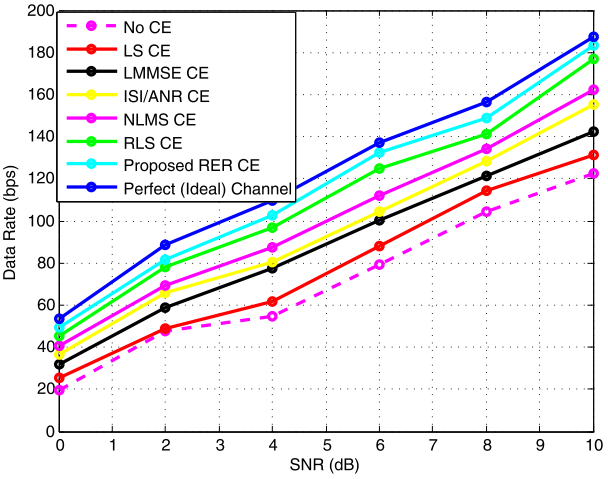

FIGURE 13. A plot of average data rate performance vs signal to noise ratio over Rician fading marine channel environment for different channel estimators.

in improved system throughput. This occurs because of the antenna selection diversity and power, where the propagating signals are more appropriately directed to the receiver end under the cooperation of more antenna applications. The performances of the estimators are further evaluated over Rayleigh and Rician fading channel conditions across the maritime radio network, where the data rates analysed over both channel conditions are presented as shown in Fig. 13 and Fig. 14 respectively. According to the results obtained from Fig. 13, it is certainly observed that CE can be adopted for aggrandising the QoS and QoE of pelagic networks where it is demonstrated that the proposed RER technique can better track the CIR of maritime radio systems for meaningful decision-making procedures over the receiving end of the communication network. This is because higher data rate transmissions and lower MSE can be achieved using this carefully designed scheme in comparison to other existing methods. Specifically, it is observed from Fig. 14 that the proposed RER estimator similarly shows a performance gain of just about 1 dB SNR at a data rate of 100 bps when compared to conventional RLS while the estimator demonstrates a gain of almost 4 dB SNR when compared to traditional LS methods.

The marine QoS can be evaluated based on the outage probability and the QoS-guaranteed probability at various SNR ranges considering the effects of massive antenna deplorations over service clouds to enhance the QoE of thalassic users. The simulated and theoretical outage probability of transmission from ship to coastline base station is evaluated as applicable to oceanographic communications as shown in Fig. 15 for different values of SNRs and DAs per service cloud over Rayleigh and Rician fading channel propagation. The chart presented in Fig. 16 also show a comparative graphical analysis of the system outage probabilities at different levels of SNR values assuming both LoS and NLoS signal transmissions giving different DAs per service cloud. The QoS-guaranteed probability is also evaluated over

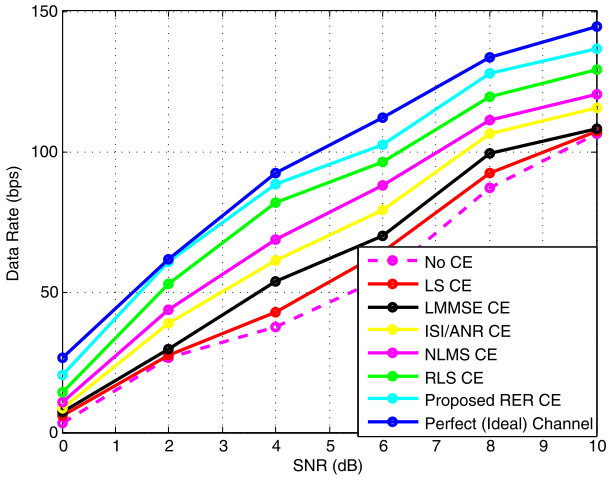

FIGURE 14. A plot of average data rate performance vs signal to noise ratio over Rayleigh fading marine channel environment for different channel estimators.

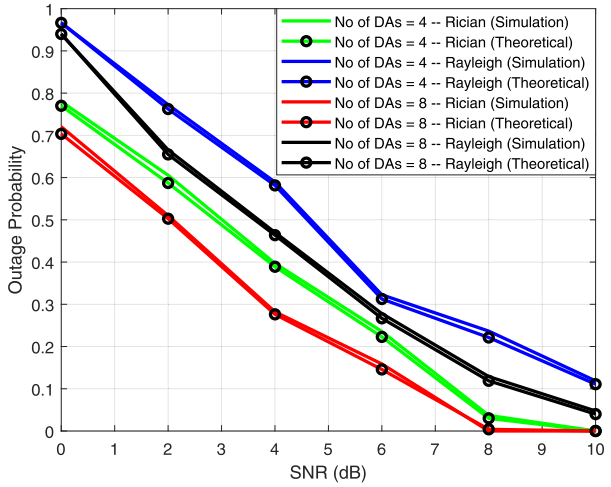

FIGURE 15. A plot of transmission outage probability vs signal to noise ratio over Rician and Rayleigh propagation for 4 and 8 directional antenna per service cloud.

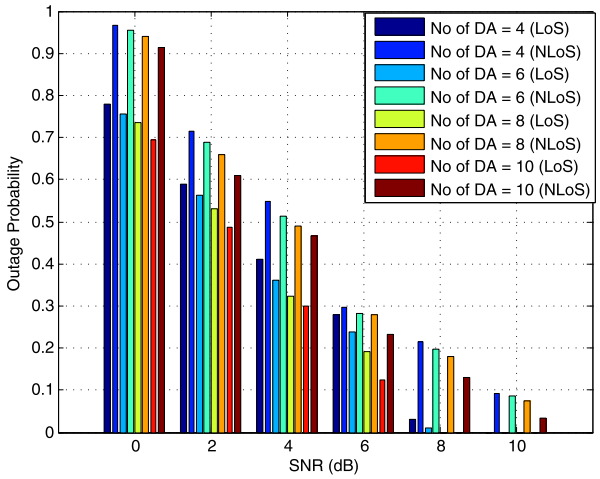

FIGURE 16. A plot of average probability of outage vs signal to noise ratio over LoS and NLoS propagation at different numbers of directional antenna per service cloud.

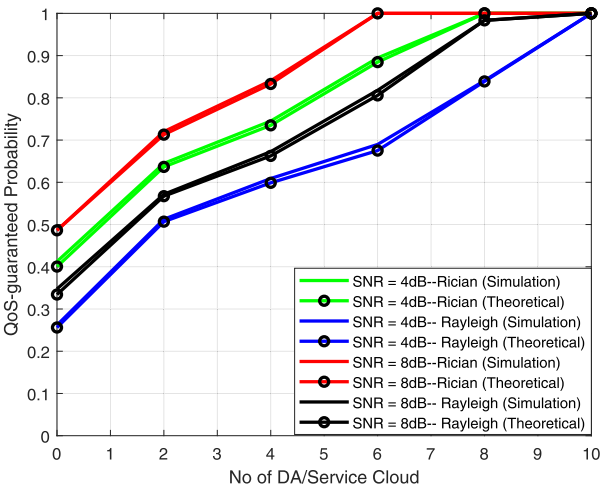

FIGURE 17. A plot of QoS guaranteed probability vs number of directional antenna per service cloud over Rician and Rayleigh fading for signal to noise ratio of 4 and 8 dB.

different SNR values and DAs per service cloud over similar channel models as shown in Fig. 17 respectively. Results obtained demonstrate that the transmission outage probability increases as the SNR values decreases and as the number of DAs serving the pelagic communication system decreases. It is also shown that the transmission of marine signals over Rayleigh fading channels increases the transmission outage probabilities due to the unpropitious effects of the environmental conditions thereby, leading to poorer signal reception at the coast-line BS during decision-making procedures. Hence, in such conditions, marine users are more likely to experience unwanted transaction delays, economic loses in addition to seaport congestions and probable collisions. It can also be deduced from Fig. 17 that the use of monumental antennas can sharply increase the QoS-guaranteed probability of marine users especially at higher SNR values. Hence, transmissions over 8 dB Rician fading channel will converge faster than transmissions over its Rayleigh fading counterpart. Thus, fewer DAs will be required for optimal signal transmissions over LoS propagations as the network QoS-guaranteed probability will converge when the number of DAs employed per service cloud is 6 as compared to 9 for its NLoS counterpart when the SNR is in this region of 8 dB. Finally, it is demonstrated in Fig. 18 and 19 that the QoE of marine users can be improved with appropriate CE techniques. In these figures, it is observed that the application of appropriate CE methods can significantly reduce the transmission outage probabilities which subsequently strengthens the reception of aggregated CH signals at the BS of the maritime network thus, improving the QoS and QoE of the marine network as a result. From the curves, adopting the proposed RER CE method can considerably reduce the system outage probability in comparison to other techniques, since the receiver will have much knowledge of the actual conditions of the maritime environment before and during the transmission of the aggregated ship-implanted MUE signals.

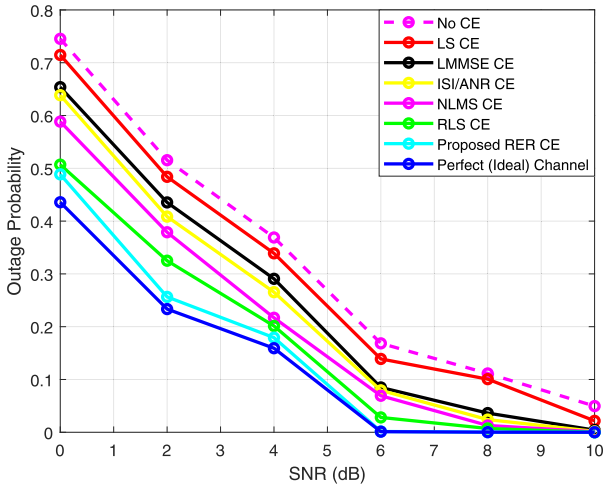

FIGURE 18. A plot of average probability of outage performance vs signal to noise ratio over Rician fading marine channel environment for different channel estimators.

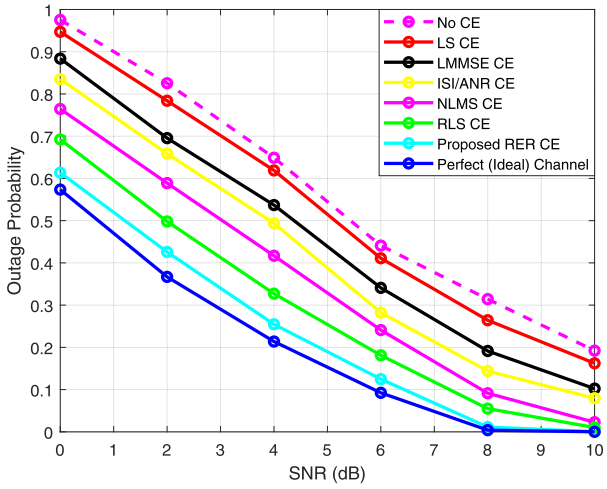

FIGURE 19. A plot of average probability of outage performance vs signal to noise ratio over Rayleigh fading marine channel environment for different channel estimators.

Similarly, marine communication systems will experience a higher probability of transmission outage in a small-scale Rayleigh fading environment over their Rician counterparts. At higher SNR values, the outage probabilities across both fading channels reduce proportionately.

VII. FINDINGS AND POSSIBLE RESEARCH DIRECTIONS

The penultimate section presents an elaborate discussion of results obtained for improving maritime communication networks. This section provides an overall summary of research findings from this work in addition to possible future research directions for the development of IoMT.

To begin with, it can be observed that the relative CE performances of the estimation schemes when signals propagate under slow fading channel environmental conditions are noticeably superior in comparison to system performances of corresponding channels that are characterised by fast fading CIR scenarios. This is because the propagating CH information sent from the vessel to the on-shore mounted base station can be easily trailed when the CSI oscillates slowly over a given period of time as compared to the expeditious changes that mark the CSI characteristics of fast fading channel propagation. Another preeminent trend that is worth noting is that the MSE performances of the proposed CE schemes decrease steadily with increases in the SNR values since the varying characteristics of the fading channel will be better tracked when the signal quality is way higher than the unwanted effects of the channel noises. More so, the results obtained proved that the adaptive schemes show better estimation performances for marine signal tracking in comparison with their linear counterparts because they recursively obtain the CIR that minimizes a cost function, which relates to the previous estimates and the CH information. Furthermore, simulation results illustrate that as the number of DA increases per service cloud over offshore navigating vessels, the data rate increases proportionately over the communication network since the effects of environmental interference are drastically reduced which is further improved by CE. Additionally, it is inferred that the data rate improves as the number of DAs per service cloud and SNR values increases over LoS and NLoS communication scenarios in both situations where the CH-DA transmission is enabled over Rician and Rayleigh fading channels respectively. Conversely, the outage probabilities of marine networks decreases as the number of service cloud DAs increase at rising SNR values while the QoS-guaranteed probability rises with increase in costline mounted DAs even at extreme transmission conditions.

At this point, it is extremely important to note that the development of marine IoT-enabled communication technologies is currently an open research area that is worthy to draw the attention of numerous researchers and scholars in the field, where the safety, security, energy efficiency and environmental sustainabilities of nautical communication networks can be tremendously considered and improved. There is still need to develop novel IoT architectures which are capable of integrating numerous enabling technologies and heterogeneous services, so as to provide efficient network interoperability in order to drastically mitigate the detrimental effects and conditions experienced during marine explorations. As such, developing unorthodox communication technologies/ algorithms based on software-defined networking (SDN), network functions virtualization (NFV), gateway solutions and content-centric networking (CCN) etc., can still be considered for enhancing the designs of marine hardware architectures for the IoMTs in order to improve the overall network transmission data rates, spectral efficiencies, channel estimation, navigation security/ access control and the wholistic QoS-guaranteed probabilities of oceanographic communications. More so, the development of software architectures that will enhance computation, mining, unsupervised and reinforcement learning, and aggregation of marine data with huge volumes, varieties and speed is still an open research issue for nautical communication systems.

As such, the extensive deploration and improvement of fog and cloud computing technologies [31]–[33] can go a mile to significantly support nautical explorations ranging from oil and gas drilling/maintenance to maritime cargo transportations and to underwater navigation/explorations etc. Also, developing low complexity CE methods that optimise the QoS of marine networks in addition to enabling wider network coverages is an open research area awaiting exploitation by enthusiastic researchers. Finally, it is a known fact that the continuous maintenance of beam angle during practical operations of directional antennas is extremely challenging. As such, investigating the performances and operations of thalassic networks when the beam adaptation fails between the sea-mounted control centre and the on-shore position marine vessel will be an interesting research area worth considering by research experts and practitioners in the field.

VIII. CONCLUSION

Channel estimation can be employed to predict the transmission and reception of saltwater communications. This research shows that adaptive estimators in comparison to their linear counterparts offer better estimation of channel properties which consequently give rise to ameliorate signal receptions for useful maritime decision making procedures. Specifically, the proposed RER CE scheme offers better MSE performance, estimation stability and faster convergence rate in comparison to the conventional RLS CE method assuming both slow and fast fading marine network transmissions. Thus, the RER CE algorithm is recommended for use in maritime radio networks for combating the dynamics of nautical channels especially under frequent heavy shadowing (Non-LOS) maritime communication scenarios. Hence, it is concluded that the channel dynamics of maritime fading systems are better combated using the proposed adaptive RER estimation technique as compared to other considered estimation schemes due to the provision of a reweighting attractor that shrinks the estimation errors in addition to provision of additional system stability while the proposed ISI/ANR improves the estimation capabilities of marine networks in comparison to other evaluated linear estimators. Finally, it is also concluded that network data rates and user QoS experiences increases as more DAs are deployed for marine communications at higher SNRs.

APPENDIX

A. PROOF OF PROPOSED ISI/ANR CHANNEL ESTIMATE

The PDF of the received signal according to (13) is given as:

$$f_Y(y[\ddot{D}_i, i]) = \frac{1}{\sqrt{2\pi\sigma_w^2}} \times \exp\left(-\frac{1}{2\sigma_w^2}\left(y[\ddot{D}_i, i] - C[\ddot{D}_i, i]g[\ddot{D}_i, i]\right)^2\right) \quad \text{(A-1)}$$

If the channel noise $w[\ddot{D}_i, i]$ are independent and identically distributed (iid), then the received observation $y[\ddot{D}_i, i]$ will also be iid such that the joint PDF of the received signal is expressed as a product of the individual PDFs of the received signal observation [23]. It is important to note that the likelihood function of a channel estimate $\Lambda_L[y[\ddot{D}_i, i], C]$ is denoted as the joint PDF of the received signal vector which is specified by the CIR. This is simply derived as the product of the PDF of individual received observation shown as:

$$\begin{aligned}\Lambda_L[y[\ddot{D}_i, i], C] &= f_{Y(1)Y(2)\ldots Y(\ddot{d})}[y(1), y(2), \ldots, y(\ddot{d})]) \\ &= f_{Y(1)}y(1) \times f_{Y(2)}y(2) \times \ldots \times f_{Y(\ddot{d})}y(\ddot{d})\end{aligned} \quad \text{(A-2)}$$

where the PDF of individual sample of received observation is given in (13). Hence, the joint PDF of received observation $\Lambda_L[y[\ddot{D}_i, i], C]$ according to the Gaussian PDF can be expressed as in (A-3).

If the logarithm of the likelihood function according to (A-3) is evaluated, then the log-likelihood function of the unknown channel $\Lambda_{\log L}[y[\ddot{D}_i, i], C]$ can be represented as:

$$\begin{aligned}\Lambda_{\log L}[y[\ddot{D}_i, i], C] &= \log_e\left(\Lambda_L[y[\ddot{D}_i, i], C]\right) \\ &= \ln\left(\Lambda_L[y[\ddot{D}_i, i], C]\right) = \ln\left(\left(\frac{1}{\sqrt{2\pi\sigma_w^2}}\right)^{\ddot{d}} \exp\left(-\frac{1}{2\sigma_w^2} \times \sum_{\ddot{k}=1}^{\ddot{d}} \left(y[\ddot{k}] - C[\ddot{k}]g[\ddot{k}]\right)^2\right)\right) \\ &= \ln\left(\left(\frac{1}{\sqrt{2\pi\sigma_w^2}}\right)^{\ddot{d}}\right)\end{aligned}$$

$$\begin{aligned}&f_{Y(1)Y(2)\ldots Y(\ddot{d})}[y(1), y(2), \ldots, y(\ddot{d})]) \\ &= \frac{1}{\sqrt{2\pi\sigma_w^2}} \exp\left(-\frac{1}{2\sigma_w^2}\left(y[1] - C[1]g[1]\right)^2\right) \times \frac{1}{\sqrt{2\pi\sigma_w^2}} \exp\left(-\frac{1}{2\sigma_w^2}\left(y[2] - C[2]g[2]\right)^2\right) \\ &\quad \ldots \frac{1}{\sqrt{2\pi\sigma_w^2}} \exp\left(-\frac{1}{2\sigma_w^2}\left(y[\ddot{d}] - C[\ddot{d}]g[\ddot{d}]\right)^2\right)\end{aligned}$$

hence,

$$\Lambda_L[y[\ddot{D}_i, i], C] = \left(\frac{1}{\sqrt{2\pi\sigma_w^2}}\right)^{\ddot{d}} \exp\left(-\frac{1}{2\sigma_w^2} \sum_{\ddot{k}=1}^{\ddot{d}} \left(y[\ddot{k}] - C[\ddot{k}]g[\ddot{k}]\right)^2\right) \quad \text{(A-3)}$$

$$+\ln\left(\exp\left(-\frac{1}{2\sigma_w^2}\sum_{\ddot{k}=1}^{\ddot{d}}\left(y[\ddot{k}]-C[\ddot{k}]g[\ddot{k}]\right)^2\right)\right)$$
$$=\ddot{d}\ln\left(\frac{1}{\sqrt{2\pi\sigma_w^2}}\right)-\left(\frac{1}{2\sigma_w^2}\sum_{\ddot{k}=1}^{\ddot{d}}\left(y[\ddot{k}]-C[\ddot{k}]g[\ddot{k}]\right)^2\right) \tag{A-4}$$

The maximum likelihood estimate of the channel fading coefficients $\hat{C}_{ML}[\ddot{D}_i, i]$ is obtained by evaluating the parameter that maximizes the log-likelihood function expressed in (A-4). Hence,

$$\hat{C}_{ML}[\ddot{D}_i, i] = \max \Lambda_{\log L}[y[\ddot{D}_i, i], C]$$

The expression $\left(\Lambda_{\log L}[y[\ddot{D}_i, i], C]\right)$ is maximized if

$$=\frac{\partial\left(\Lambda_{\log L}[y[\ddot{D}_i, i], C]\right)}{\partial C}=0,\quad \forall\ \ddot{k}=1,2,\ldots,\ddot{d}$$

Thus,

$$\frac{\partial\left(\ddot{d}\ln\left(\frac{1}{\sqrt{2\pi\sigma_w^2}}\right)\right)}{\partial C}-\frac{\partial\left(\frac{1}{2\sigma_w^2}\sum_{\ddot{k}=1}^{\ddot{d}}\left(y[\ddot{k}]-C[\ddot{k}]g[\ddot{k}]\right)^2\right)}{\partial C}$$
$$=\left(-\frac{1}{2\sigma_w^2}\right)\times 2\left(\sum_{\ddot{k}=1}^{\ddot{d}}\left(y[\ddot{k}]-C[\ddot{k}]g[\ddot{k}]\right)\times\left(-g[\ddot{k}]\right)\right.$$
$$=0\implies\sum_{\ddot{k}=1}^{\ddot{d}}\left(y[\ddot{k}]-C[\ddot{k}]g[\ddot{k}]\right)\times\left(g[\ddot{k}]\right)=0$$
$$\therefore\sum_{\ddot{k}=1}^{\ddot{d}}\left(y[\ddot{k}]g[\ddot{k}]-C[\ddot{k}]g^2[\ddot{k}]\right)=0,\quad \text{hence,}$$
$$\sum_{\ddot{k}=1}^{\ddot{d}}y[\ddot{k}]g[\ddot{k}]-\sum_{\ddot{k}=1}^{\ddot{d}}C[\ddot{k}]g^2[\ddot{k}]=0$$
or
$$\sum_{\ddot{k}=1}^{\ddot{d}}C[\ddot{k}]g^2[\ddot{k}]=\sum_{\ddot{k}=1}^{\ddot{d}}y[\ddot{k}]g[\ddot{k}]$$
$$C[\ddot{k}]=\frac{\sum_{\ddot{k}=1}^{\ddot{d}}y[\ddot{k}]g[\ddot{k}]}{g^2[\ddot{k}]}\qquad\forall\ \ddot{k}=1,2,\ldots,\ddot{d} \tag{A-5}$$

Finally,

$$\hat{C}_{ML}[\ddot{D}_i, i]=\text{diag}\left(C[1], C[2], \ldots, C[\ddot{d}]\right) \tag{A-6}$$

where $C[\ddot{k}]$ is given by A-5. The derived expression in (A-5) is equivalent to the ML-based CE presented in (24) which is further improved to obtain the ISI/ANR estimate. Here, the interference and noise components of the marine channel are considered and normalised with the Frobenius norm of the ML channel coefficients. This gives the ISI/ANR technique an edge over traditional ML method as the later does not take into consideration, a combination of both unwanted channel phenomena.

B. PROOF OF PROPOSED RER CHANNEL ESTIMATE

The product $\left[(g[\ddot{D}_i, i]g^H[\ddot{D}_i, i])\right]$ as obtained from $\ddot{d}\times\ddot{d}$ correlation matrix can be re-weighted by an exponential factor given as $\breve{\lambda}^{\ddot{D}_i-i}$. As such, the $\ddot{d}\times\ddot{d}$ correlation matrix for deriving an RLS CE is presented as:

$$\bar{\boldsymbol{\Upsilon}}_{RLS}[\ddot{D}_i, i]=\sum_{i=1}^{\ddot{D}_i}\breve{\lambda}^{\ddot{D}_i-i}\left(g[\ddot{D}_i, i]g^H[\ddot{D}_i, i]\right) \tag{B-1}$$

From the expression in (B-1), if $(\ddot{D}_i=1)$ is isolated from the summation, then the RLS-based correlation matrix can be written as:

$$\bar{\boldsymbol{\Upsilon}}_{RLS}[\ddot{D}_i, i]=\breve{\lambda}\left[\sum_{i=1}^{\ddot{D}_i-1}\breve{\lambda}^{\ddot{D}_i-i-1}\left(g[\ddot{D}_i, i]g^H[\ddot{D}_i, i]\right)\right]$$
$$+\left(g[\ddot{D}_i, i]g^H[\ddot{D}_i, i]\right) \tag{B-2}$$

Comparing the expressions (B-1) and (B-2), the RLS-based correlation matrix based on previous estimate $\left(\bar{\boldsymbol{\Upsilon}}_{RLS}[\ddot{D}_i-1, i]\right)$ can then be formulated as:

$$\bar{\boldsymbol{\Upsilon}}_{RLS}[\ddot{D}_i-1, i]=\sum_{i=1}^{\ddot{D}_i-1}\breve{\lambda}^{\ddot{D}_i-i-1}\left(g[\ddot{D}_i, i]g^H[\ddot{D}_i, i]\right) \tag{B-3}$$

Substituting (B-3) into (B-2) gives the expression in (B-4) which is used for updating the deterministic correlation matrix:

$$\bar{\boldsymbol{\Upsilon}}_{RLS}^{-1}[\ddot{D}_i, i]=\breve{\lambda}\bar{\boldsymbol{\Upsilon}}_{RLS}[\ddot{D}_i-1, i]+g[\ddot{D}_i, i]g^H[\ddot{D}_i, i] \tag{B-4}$$

The use of matrix inversion lemma can be adopted for deriving the RLS-based channel estimate where the inverse autocorrelation matrix $\bar{\boldsymbol{\Upsilon}}_{RLS}^{-1}[\ddot{D}_i, i]$ is obtained. The properties of this lemma is summarized as follows. Let two positive-definite $\ddot{D}_i\times\ddot{D}_i$ matrix be represent as $\ddot{\mathbf{Y}}$ and $\ddot{\mathbf{B}}$ such that they are related by:

$$\ddot{\mathbf{Y}}=\ddot{\mathbf{B}}^{-1}+\ddot{\mathbf{U}}\ddot{\mathbf{V}}^{-1}\ddot{\mathbf{U}}^H \tag{B-5}$$

In (B-5), $\ddot{\mathbf{U}}$ is a $\ddot{D}_i\times\ddot{E}_i$ matrix while $\ddot{\mathbf{V}}$ is an $\ddot{E}_i\times\ddot{E}_i$ small positive-definite matrix. From this expression, the matrix inversion lemma can then be used to obtain the inverse of $\ddot{\mathbf{Y}}$ which is given as:

$$\ddot{\mathbf{Y}}^{-1}=\ddot{\mathbf{B}}-\ddot{\mathbf{B}}\ddot{\mathbf{U}}\left(\ddot{\mathbf{V}}+\ddot{\mathbf{U}}^H\ddot{\mathbf{B}}\ddot{\mathbf{U}}\right)^{-1}\ddot{\mathbf{U}}^H\ddot{\mathbf{B}} \tag{B-6}$$

The product of (B-5) and (B-6) gives unity. As such, from the matrix inversion lemma, the RLS inverse correlation matrix $\left(\bar{\boldsymbol{\Upsilon}}_{RLS}^{-1}[\ddot{D}_i, i]\right)$ can be obtained if the following substitutions below are inserted into (B-6) [20]:
$\ddot{\mathbf{Y}}=\bar{\boldsymbol{\Upsilon}}_{RLS}^{-1}[\ddot{D}_i, i], \ddot{\mathbf{U}}=g[\ddot{D}_i, i], \ddot{\mathbf{B}}^{-1}=\breve{\lambda}\bar{\Upsilon}_{RLS}[\ddot{D}_i-1, i], \ddot{\mathbf{V}}=1$ Thus, $\left(\bar{\boldsymbol{\Upsilon}}_{RLS}^{-1}[\ddot{D}_i, i]\right)$ can be obtained as the expression in (B-7), as shown at the bottom of the next page.

Let the inverse autocorrelation matrix $\bar{\boldsymbol{\Upsilon}}_{RLS}^{-1}[\ddot{D}_i, i]$ for computational convenience be denoted as $\hat{\boldsymbol{\rho}}_{RLS}[\ddot{D}_i, i]$ such that:

$$\hat{\boldsymbol{\rho}}_{RLS}[\ddot{D}_i, i]=\bar{\boldsymbol{\Upsilon}}_{RLS}^{-1}[\ddot{D}_i, i] \tag{B-8}$$

As such;

$$\hat{\boldsymbol{\rho}}_{RLS}[\ddot{D}_i - 1, i] = \bar{\boldsymbol{\Upsilon}}^{-1}_{RLS}[\ddot{D}_i - 1, i] \tag{B-9}$$

From the expression in (B-7), if the gain vector is represented according to (31), then this (gain) vector can be represented using the notation given in (B-9) as:

$$\vec{\eth}[\ddot{D}_i, i] = \frac{\breve{\lambda}^{-1}\hat{\boldsymbol{\rho}}_{RLS}[\ddot{D}_i - 1, i]g[\ddot{D}_i, i]}{1 + g^H[\ddot{D}_i, i]\breve{\lambda}^{-1}\hat{\boldsymbol{\rho}}_{RLS}[\ddot{D}_i - 1, i]g[\ddot{D}_i, i]} \tag{B-10}$$

Hence, the inverse autocorrelation matrix $\hat{\boldsymbol{\rho}}_{RLS}[\ddot{D}_i, i]$ can be derived by simply substituting (B-8), (B-9) and (B-10) into the expression in (B-7). Thus,

$$\begin{aligned}\hat{\boldsymbol{\rho}}_{RLS}[\ddot{D}_i, i] &= \breve{\lambda}^{-1}\hat{\boldsymbol{\rho}}_{RLS}[\ddot{D}_i - 1, i] \\ &\quad - \breve{\lambda}^{-1}\vec{\eth}[\ddot{D}_i, i]g^H[\ddot{D}_i, i]\hat{\boldsymbol{\rho}}_{RLS}[\ddot{D}_i - 1, i]\end{aligned} \tag{B-11}$$

It is worth noting that (B-11) can also be given as:

$$\begin{aligned}\bar{\boldsymbol{\Upsilon}}^{-1}_{RLS}[\ddot{D}_i - 1, i] &= \breve{\lambda}^{-1}\bar{\boldsymbol{\Upsilon}}^{-1}_{RLS}[\ddot{D}_i - 1, i] \\ &\quad - \breve{\lambda}^{-1}\vec{\eth}[\ddot{D}_i, i]g^H[\ddot{D}_i, i]\bar{\boldsymbol{\Upsilon}}^{-1}_{RLS}[\ddot{D}_i - 1, i]\end{aligned} \tag{B-12}$$

The expression in (B-10) can further be simplified as follows:

$$\begin{aligned}&\vec{\eth}[\ddot{D}_i, i]\Big(1 + g^H[\ddot{D}_i, i]\lambda^{-1}\hat{\boldsymbol{\rho}}_{RLS}[\ddot{D}_i - 1, i]g[\ddot{D}_i, i]\Big) \\ &\quad = \breve{\lambda}^{-1}\hat{\boldsymbol{\rho}}_{RLS}[\ddot{D}_i - 1, i]g[\ddot{D}_i, i] \\ &\big(\vec{\eth}[\ddot{D}_i, i] + \vec{\eth}[\ddot{D}_i, i]g^H[\ddot{D}_i, i]\breve{\lambda}^{-1}\hat{\boldsymbol{\rho}}_{RLS}[\ddot{D}_i - 1, i]g[\ddot{D}_i, i]\big) \\ &\quad = \breve{\lambda}^{-1}\hat{\boldsymbol{\rho}}_{RLS}[\ddot{D}_i - 1, i]g[\ddot{D}_i, i] - \vec{\eth}[\ddot{D}_i, i] \\ &\quad \Longrightarrow \vec{\eth}[\ddot{D}_i, i] = \breve{\lambda}^{-1}\hat{\boldsymbol{\rho}}_{RLS}[\ddot{D}_i - 1, i]g[\ddot{D}_i, i] \\ &\qquad - \vec{\eth}[\ddot{D}_i, i]g^H[\ddot{D}_i, i]\breve{\lambda}^{-1}\hat{\boldsymbol{\rho}}_{RLS}[\ddot{D}_i - 1, i]g[\ddot{D}_i, i] \\ &\qquad \vec{\eth}[\ddot{D}_i, i] = g[\ddot{D}_i, i]\Big[\breve{\lambda}^{-1}\hat{\boldsymbol{\rho}}_{RLS}[\ddot{D}_i - 1, i] \\ &\qquad - \vec{\eth}[\ddot{D}_i, i]g^H[\ddot{D}_i, i]\breve{\lambda}^{-1}\hat{\boldsymbol{\rho}}_{RLS}[\ddot{D}_i - 1, i]\Big]\end{aligned} \tag{B-13}$$

Inserting the expression in (B-11) into (B-13),

$$\vec{\eth}[\ddot{D}_i, i] = \hat{\boldsymbol{\rho}}_{RLS}[\ddot{D}_i, i]g[\ddot{D}_i, i] \tag{B-14}$$

When the performance index according to (29) attains its minimum value, then the optimum RLS channel estimate can be obtained using the expression in (B-15) [20].

$$\hat{C}_{RLS}[\ddot{D}_i, i] = \bar{\boldsymbol{\Upsilon}}^{-1}_{RLS}[\ddot{D}_i, i]\ddot{\boldsymbol{\omega}}[\ddot{D}_i, i] \tag{B-15}$$

where $\ddot{\boldsymbol{\omega}}$ is a $\ddot{D}_i \times 1$ cross-correlation vector between $g[\ddot{D}_i, i]$ and $y[\ddot{D}_i, i]$ which can be compared to (B-1) such that $(*)$ represents complex conjugation by the expression:

$$\ddot{\boldsymbol{\omega}}[\ddot{D}_i, i] = \sum_{i=1}^{\ddot{D}_i}\breve{\lambda}^{\ddot{D}_i - i}\Big(g[\ddot{D}_i, i]y^*[\ddot{D}_i, i]\Big) \tag{B-16}$$

The notation $\ddot{\boldsymbol{\omega}}[\ddot{D}_i, i]$ can also be similarly expressed in comparison with the auto correlation matrix according to (B-4). Thus,

$$\ddot{\boldsymbol{\omega}}[\ddot{D}_i, i] = \breve{\lambda}\ddot{\boldsymbol{\omega}}[\ddot{D}_i - 1, i] + g[\ddot{D}_i, i]y^*[\ddot{D}_i, i] \tag{B-17}$$

Substituting B-17 into B-15, the following expressions are obtained.

$$\begin{aligned}&\hat{C}_{RLS}[\ddot{D}_i, i] \\ &\quad = \bar{\boldsymbol{\Upsilon}}^{-1}_{RLS}[\ddot{D}_i, i]\Big[\breve{\lambda}\ddot{\boldsymbol{\omega}}[\ddot{D}_i - 1, i] + g[\ddot{D}_i, i]y^*[\ddot{D}_i, i]\Big] \\ &\quad = \hat{\boldsymbol{\rho}}_{RLS}[\ddot{D}_i, i]\Big[\breve{\lambda}\ddot{\boldsymbol{\omega}}[\ddot{D}_i - 1, i] + g[\ddot{D}_i, i]y^*[\ddot{D}_i, i]\Big] \\ &\quad = \hat{\boldsymbol{\rho}}_{RLS}[\ddot{D}_i, i]\ddot{\boldsymbol{\omega}}[\ddot{D}_i - 1, i] + \hat{\boldsymbol{\rho}}_{RLS}[\ddot{D}_i, i]g[\ddot{D}_i, i]y^*[\ddot{D}_i, i]\end{aligned} \tag{B-18}$$

Substituting (B-11) into (B-18) yields

$$\begin{aligned}&\hat{C}_{RLS}[\ddot{D}_i, i] \\ &= \breve{\lambda}\big[\breve{\lambda}^{-1}\hat{\boldsymbol{\rho}}_{RLS}[\ddot{D}_i - 1, i] \\ &\quad - \breve{\lambda}^{-1}\vec{\eth}[\ddot{D}_i, i]g^H[\ddot{D}_i, i]\hat{\boldsymbol{\rho}}_{RLS}[\ddot{D}_i - 1, i]\big]\ddot{\boldsymbol{\omega}}[\ddot{D}_i - 1, i] \\ &\quad + \hat{\boldsymbol{\rho}}_{RLS}[\ddot{D}_i, i]g[\ddot{D}_i, i]y^*[\ddot{D}_i, i] \\ &= \big[\hat{\boldsymbol{\rho}}_{RLS}[\ddot{D}_i - 1, i] - \vec{\eth}[\ddot{D}_i, i]g^H[\ddot{D}_i, i]\hat{\boldsymbol{\rho}}_{RLS}[\ddot{D}_i - 1, i]\big]\ddot{\boldsymbol{\omega}} \\ &\quad \times [\ddot{D}_i - 1, i] + \hat{\boldsymbol{\rho}}_{RLS}[\ddot{D}_i, i]g[\ddot{D}_i, i]y^*[\ddot{D}_i, i] \\ &= \hat{\boldsymbol{\rho}}_{RLS}[\ddot{D}_i - 1, i]\ddot{\boldsymbol{\omega}}[\ddot{D}_i - 1, i] \\ &\quad - \vec{\eth}[\ddot{D}_i, i]g^H[\ddot{D}_i, i]\hat{\boldsymbol{\rho}}_{RLS}[\ddot{D}_i - 1, i]\ddot{\boldsymbol{\omega}}[\ddot{D}_i - 1, i] \\ &\quad + \hat{\boldsymbol{\rho}}_{RLS}[\ddot{D}_i, i]g[\ddot{D}_i, i]y^*[\ddot{D}_i, i]\end{aligned}$$

$$\begin{aligned}\bar{\boldsymbol{\Upsilon}}^{-1}_{RLS}[\ddot{D}_i, i] &= \Big[\breve{\lambda}\bar{\boldsymbol{\Upsilon}}_{RLS}[\ddot{D}_i - 1, i]\Big]^{-1} \\ &\quad - \Big(\big[\breve{\lambda}\bar{\boldsymbol{\Upsilon}}_{RLS}[\ddot{D}_i - 1, i]\big]^{-1}g[\ddot{D}_i, i]\big(1 + g^H[\ddot{D}_i, i]\big[\breve{\lambda}\bar{\boldsymbol{\Upsilon}}_{RLS}[\ddot{D}_i - 1, i]\big]^{-1}g[\ddot{D}_i, i]\big)^{-1}\Big)g^H[\ddot{D}_i, i] \\ &\quad \times \big[\breve{\lambda}\bar{\boldsymbol{\Upsilon}}_{RLS}[\ddot{D}_i - 1, i]\big]^{-1} = \breve{\lambda}^{-1}\bar{\boldsymbol{\Upsilon}}^{-1}_{RLS}[\ddot{D}_i - 1, i] \\ &\quad - \Big(\breve{\lambda}^{-1}\bar{\boldsymbol{\Upsilon}}^{-1}_{RLS}[\ddot{D}_i - 1, i]g[\ddot{D}_i, i]\big(1 + g^H[\ddot{D}_i, i]\breve{\lambda}^{-1}\bar{\boldsymbol{\Upsilon}}^{-1}_{RLS}[\ddot{D}_i - 1, i]g[\ddot{D}_i, i]\big)^{-1}g^H[\ddot{D}_i, i]\breve{\lambda}^{-1}\bar{\boldsymbol{\Upsilon}}^{-1}_{RLS}[\ddot{D}_i - 1, i]\Big) \\ &= \breve{\lambda}^{-1}\bar{\boldsymbol{\Upsilon}}^{-1}_{RLS}[\ddot{D}_i - 1, i] - \left[\frac{\breve{\lambda}^{-1}\bar{\boldsymbol{\Upsilon}}^{-1}_{RLS}[\ddot{D}_i - 1, i]g[\ddot{D}_i, i]g^H[\ddot{D}_i, i]\breve{\lambda}^{-1}\bar{\boldsymbol{\Upsilon}}^{-1}_{RLS}[\ddot{D}_i - 1, i]}{1 + g^H[\ddot{D}_i, i]\breve{\lambda}^{-1}\bar{\boldsymbol{\Upsilon}}^{-1}_{RLS}[\ddot{D}_i - 1, i]g[\ddot{D}_i, i]}\right] \\ \Longrightarrow \bar{\boldsymbol{\Upsilon}}^{-1}_{RLS}[\ddot{D}_i, i] &= \breve{\lambda}^{-1}\bar{\boldsymbol{\Upsilon}}^{-1}_{RLS}[\ddot{D}_i - 1, i] - \left[\frac{\breve{\lambda}^{-2}\bar{\boldsymbol{\Upsilon}}^{-1}_{RLS}[\ddot{D}_i - 1, i]g[\ddot{D}_i, i]g^H[\ddot{D}_i, i]\bar{\boldsymbol{\Upsilon}}^{-1}_{RLS}[\ddot{D}_i - 1, i]}{1 + g^H[\ddot{D}_i, i]\breve{\lambda}^{-1}\bar{\boldsymbol{\Upsilon}}^{-1}_{RLS}[\ddot{D}_i - 1, i]g[\ddot{D}_i, i]}\right]\end{aligned} \tag{B-7}$$

$$= \bar{\boldsymbol{\Upsilon}}_{RLS}^{-1}[\ddot{D}_i - 1, i]\ddot{\boldsymbol{\omega}}[\ddot{D}_i - 1, i] - \vec{\eth}[\ddot{D}_i, i]g^H[\ddot{D}_i, i]\bar{\boldsymbol{\Upsilon}}_{RLS}^{-1}[\ddot{D}_i - 1, i]\ddot{\boldsymbol{\omega}}[\ddot{D}_i - 1, i] + \hat{\boldsymbol{\rho}}_{RLS}[\ddot{D}_i, i]g[\ddot{D}_i, i]y^*[\ddot{D}_i, i] \quad \text{(B-19)}$$

Similarly to the expression in (B-15), the previous estimate can be formulated as:

$$\hat{C}[\ddot{D}_i - 1, i] = \bar{\boldsymbol{\Upsilon}}_{RLS}^{-1}[\ddot{D}_i - 1, i]\ddot{\boldsymbol{\omega}}[\ddot{D}_i - 1, i] \quad \text{(B-20)}$$

Substituting this expression of B-20 into (B-19) yields:

$$\hat{C}_{RLS}[\ddot{D}_i, i] = \hat{C}[\ddot{D}_i - 1, i] - \vec{\eth}[\ddot{D}_i, i]g^H[\ddot{D}_i, i] . \hat{C}[\ddot{D}_i - 1, i] + \hat{\boldsymbol{\rho}}_{RLS}[\ddot{D}_i, i]g[\ddot{D}_i, i]y^*[\ddot{D}_i, i] \quad \text{(B-21)}$$

Inserting the expression in (B-14) into (B-21) yields:

$$\begin{aligned}\hat{C}_{RLS}[\ddot{D}_i, i] &= \hat{C}[\ddot{D}_i - 1, i] - \vec{\eth}[\ddot{D}_i, i]g^H[\ddot{D}_i, i] . \hat{C}[\ddot{D}_i - 1, i] + \vec{\eth}[\ddot{D}_i, i]y^*[\ddot{D}_i, i] \\ &= \hat{C}[\ddot{D}_i - 1, i] + \vec{\eth}[\ddot{D}_i, i]\big[y^*[\ddot{D}_i, i] - g^H[\ddot{D}_i, i]\hat{C}[\ddot{D}_i - 1, i]\big] \quad \text{(B-22)}\end{aligned}$$

Finally, substituting the error expression of (17) into (B-22) yields the RLS channel estimate according to (32).

C. DERIVATION OF AVERAGE DATA RATE EXPRESSION

1) AVERAGE DATA RATE DERIVATION ASSUMING RAYLEIGH FADING

The data rate expression according to (37) can be further simplified as:

$$\vec{R}_i = \mathbb{E}_{C[\ddot{D}_i,i]}\left[\log_2\left(1 + \frac{\overline{E}_p\hat{\tau}_h}{\sigma_w^2}\right)\right] \quad \text{(C-1)}$$

where $\hat{\tau}_h$ is given as in (38). Considering the PDF expression represented in (39), the integral form of the data rate of vessel i can be mathematically written as:

$$\begin{aligned}\vec{R}_i &= \int_0^g \log_2\left(1 + \frac{\overline{E}_p g}{\sigma_w^2}\right) f_{\hat{\tau}_h}(g)\mathrm{d}g \\ &= \int_0^g \log_2\left(1 + \frac{\overline{E}_p g}{\sigma_w^2}\right) \sum_{k=1}^{\ddot{d}} \varpi_k(0)\zeta_k e^{-\zeta_k g}\mathrm{d}g \\ &= \sum_{k=1}^{\ddot{d}} \zeta_k \varpi_k(0) \int_0^g \log_2\left(1 + \frac{\overline{E}_p g}{\sigma_w^2}\right) e^{-\zeta_k g}\mathrm{d}g \quad \text{(C-2)}\end{aligned}$$

From the expression in (C-2), the relation in (C-3) can be defined after applying linearity property. Hence,

$$\int_0^g \log_2\left(1 + \frac{\overline{E}_p g}{\sigma_w^2}\right) e^{-\zeta_k g}\mathrm{d}g = \frac{1}{\log_e(2)} \int_0^g \left[\log_e\left(1 + \frac{\overline{E}_p g}{\sigma_w^2}\right) e^{-\zeta_k g}\right]\mathrm{d}g \quad \text{(C-3)}$$

The solution of the integral in (C-3) can be achieved using integration by parts. Solving this expression by parts yield:

$$= \left[- \frac{e^{-\zeta_k g}\log_e\left(1 + \frac{\overline{E}_p g}{\sigma_w^2}\right)}{\zeta_k} - \int_0^g - \frac{\overline{E}_p e^{-\zeta_k g}}{\zeta_k \sigma_w^2\left(1 + \frac{\overline{E}_p g}{\sigma_w^2}\right)}\mathrm{d}g\right] \quad \text{(C-4)}$$

From (C-4), the expression $\int_0^g - \frac{\overline{E}_p e^{-\zeta_k g}}{\zeta_k \sigma_w^2\left(1 + \frac{\overline{E}_p g}{\sigma_w^2}\right)}\mathrm{d}g$ can easily be solved using the concept of *exponential integrals* such that $\left[\ddot{t} = \left(\zeta_k g + \frac{\zeta_k \sigma_w^2}{\overline{E}_p}\right)\right]$. The exponential integral is a special function that consist of the ratio between an exponential function (e) and its argument generally given as $E_1(\dot{t}) = \int_{-g}^{\infty}\left(\frac{e^{-\ddot{t}}}{\ddot{t}}\right)\mathrm{d}\ddot{t}$. Thus, the solution to this expression is given as:

$$= \int_0^g - \frac{\overline{E}_p . e^{-\zeta_k g}}{\zeta_k \sigma_w^2\left(1 + \frac{\overline{E}_p g}{\sigma_w^2}\right)}\mathrm{d}g = \frac{1}{\zeta_k}\left(e^{\frac{\zeta_k \sigma_w^2}{\overline{E}_p}} E_1\left(\zeta_k g + \frac{\zeta_k \sigma_w^2}{\overline{E}_p}\right)\right) \quad \text{(C-5)}$$

Plugging (C-5) into the integral expression in (C-4), the equation in (C-4) can be simplified as in (C-6):

$$= \left[- \frac{e^{-\zeta_k g}\log_e\left(1 + \frac{\overline{E}_p g}{\sigma_w^2}\right)}{\zeta_k} - \frac{1}{\zeta_k}\left(e^{\frac{\zeta_k \sigma_w^2}{\overline{E}_p}} E_1\left(\zeta_k g + \frac{\zeta_k \sigma_w^2}{\overline{E}_p}\right)\right)\right] \quad \text{(C-6)}$$

Thus, (C-3) can be further simplified as presented in (C-7), as shown at the bottom of the page. Lastly, if the expression in (C-7), is substituted into (C-2), then the average data rate expression assuming Rayleigh fading (NLOS) propagation can be obtained as (46).

2) AVERAGE DATA RATE DERIVATION ASSUMING SHADOWED RICIAN FADING

The PDF $f_{\|C[\ddot{D}_i,i]\|^2}(g)$ can be expressed in terms of confluent hypergeometric (Kummer's) function of the first kind as [5], [30]:

$$\begin{aligned}f_{\|C[\ddot{D}_i,i]\|^2}(g) &= (2P_E)^{\left((m-1)|\ddot{D}_i|\right)} . \eta^{(m|\ddot{D}_i|-\varphi)} \times \sum_{\hat{l}=0}^{\xi}\left(\frac{g^{\varphi-\hat{l}-1}}{\Gamma(\varphi - \hat{l})} . {}_1F_1(\varphi; \varphi - \hat{l}; -\eta g) + \frac{\phi . \eta^{\hat{l}-1}}{\Gamma(\varphi - \hat{l} + 1)} . {}_1F_1(\varphi + 1; \varphi - \hat{l} + 1; -\eta g)\right)\mathrm{d}g \quad \text{(C-8)}\end{aligned}$$

$$\int_0^g \log_2\left(1 + \frac{\overline{E}_p g}{\sigma_w^2}\right) e^{-\zeta_k g}\mathrm{d}g = \frac{1}{\log_e(2)}\left[- \frac{e^{-\zeta_k g}\log_e\left(1 + \frac{\overline{E}_p g}{\sigma_w^2}\right)}{\zeta_k} - \frac{1}{\zeta_k}\left(e^{\frac{\zeta_k \sigma_w^2}{\overline{E}_p}} E_1\left(\zeta_k g + \frac{\zeta_k \sigma_w^2}{\overline{E}_p}\right)\right)\right] \quad \text{(C-7)}$$

From the expression in (41), $\ln\left(1+\bar{\gamma}g\right)=G_{2,2}^{1,2}\left(-\bar{\gamma}g\middle|\begin{matrix}1,1\\1,0\end{matrix}\right)$ while in general, ${}_1F_1(k;m;n)=\frac{\Gamma(m)}{\Gamma(k)}G_{1,2}^{1,1}\left(-n\middle|\begin{matrix}1-k\\0,1-m\end{matrix}\right)$.

The data rate expression of the Rican fading channel according to (41) can then be simplified as:

$$\begin{aligned}\vec{R}_i &= \frac{1}{\ln 2}\int_0^\infty \ln\left(1+\bar{\gamma}g\right).(2P_E)^{\left((m-1)|\ddot{D}_i|\right)}.\eta^{(m|\ddot{D}_i|-\varphi)}\\ &\times\sum_{\hat{l}=0}^{\xi}\left(\frac{g^{\varphi-\hat{l}-1}}{\Gamma(\varphi-\hat{l})}.{}_1F_1(\varphi;\varphi-\hat{l};-\eta g)\right.\\ &\left.+\frac{\phi.g^{\varphi-\hat{l}}}{\Gamma(\varphi-\hat{l}+1)}.{}_1F_1(\varphi+1;\varphi-\hat{l}+1;-\eta g)\right)\mathrm{d}g\\ &=\frac{1}{\ln 2}(2P_E)^{\left((m-1)|\ddot{D}_i|\right)}.\eta^{(m|\ddot{D}_i|-\varphi)}\\ &\times\sum_{\hat{l}=0}^{\xi}\int_0^\infty G_{2,2}^{1,2}\left(-\bar{\gamma}g\middle|\begin{matrix}1,1\\1,0\end{matrix}\right).\left[\left(\frac{g^{\varphi-\hat{l}-1}}{\Gamma(\varphi-\hat{l})}\right)\left(\frac{\Gamma(\varphi-\hat{l})}{\Gamma(\varphi)}\right)\right.\\ &\times G_{1,2}^{1,1}\left(\eta g\middle|\begin{matrix}1-\varphi\\0,1-(\varphi-\hat{l})\end{matrix}\right)\\ &+\left(\frac{\phi.g^{\varphi-\hat{l}}}{\Gamma(\varphi-\hat{l}+1)}\right)\left(\frac{\Gamma(\varphi-\hat{l}+1)}{\Gamma(\varphi+1)}\right)\\ &\left.\times G_{1,2}^{1,1}\left(\eta g\middle|\begin{matrix}1-(\varphi+1)\\0,1-(\varphi-\hat{l}+1)\end{matrix}\right)\right]\mathrm{d}g\\ &=\frac{1}{\ln 2}(2P_E)^{\left((m-1)|\ddot{D}_i|\right)}\eta^{(m|\ddot{D}_i|-\varphi)}.\\ &\times\sum_{\hat{l}=0}^{\xi}\int_0^\infty G_{2,2}^{1,2}\left(-\bar{\gamma}g\middle|\begin{matrix}1,1\\1,0\end{matrix}\right).\left[\left(\frac{g^{\varphi-\hat{l}-1}}{\Gamma(\varphi)}\right)\right.\\ &\times G_{1,2}^{1,1}\left(\eta g\middle|\begin{matrix}1-\varphi\\0,(1-\varphi+\hat{l})\end{matrix}\right)+\left(\frac{\phi.g^{\varphi-\hat{l}}}{\Gamma(\varphi+1)}\right)\\ &\left.\times G_{1,2}^{1,1}\left(\eta g\middle|\begin{matrix}-\varphi\\0,(-\varphi+\hat{l})\end{matrix}\right)\right]\mathrm{d}g \qquad \text{(C-9)}\end{aligned}$$

Bearing in mind that $g^{\varphi-\hat{l}-1}G_{1,2}^{1,1}\left(\eta g\middle|\begin{matrix}1-\varphi\\0,(1-\varphi+\hat{l})\end{matrix}\right)=\eta^{-(\varphi-\hat{l}-1)}G_{1,2}^{1,1}\left(\eta g\middle|\begin{matrix}-\hat{l}\\(\varphi-\hat{l}-1),0\end{matrix}\right)$ and that the integration of the product of two Meijer-G functions

$$\int_0^\infty G_{1,2}^{1,1}\left(\eta g\middle|\begin{matrix}-\hat{l}\\(\varphi-\hat{l}-1,0\end{matrix}\right)G_{2,2}^{1,2}\left(-\bar{\gamma}g\middle|\begin{matrix}1,1\\1,0\end{matrix}\right)\mathrm{d}g$$

is given as

$$\frac{1}{\eta}G_{4,3}^{2,3}\left(\frac{-\bar{\gamma}}{\eta}\middle|\begin{matrix}-\varphi+\hat{l}+1,1,1,0\\\hat{l},1,0\end{matrix}\right)$$

then the data rate expression of (C-9) reduces to:

$$\begin{aligned}\vec{R}_i &= \frac{1}{\ln 2}(2P_E)^{\left((m-1)|\ddot{D}_i|\right)}.\eta^{(m|\ddot{D}_i|-\varphi)}\sum_{\hat{l}=0}^{\xi}\\ &.\left[\left(\frac{\eta^{-(\varphi-\hat{l}-1)}}{\Gamma(\varphi)}\right)\int_0^\infty G_{1,2}^{1,1}\left(\eta g\middle|\begin{matrix}-\hat{l}\\(\varphi-\hat{l}-1),0\end{matrix}\right)\right.\\ &\times G_{2,2}^{1,2}\left(-\bar{\gamma}g\middle|\begin{matrix}1,1\\1,0\end{matrix}\right)\mathrm{d}g+\left(\frac{\phi.\eta^{-(\varphi-\hat{l})}}{\Gamma(\varphi+1)}\right)\int_0^\infty\\ &\left.\times G_{1,2}^{1,1}\left(\eta g\middle|\begin{matrix}1-\hat{l}\\(\varphi-\hat{l}),0\end{matrix}\right)G_{2,2}^{1,2}\left(-\bar{\gamma}g\middle|\begin{matrix}1,1\\1,0\end{matrix}\right)\mathrm{d}g\right]. \qquad \text{(C-10)}\\ &=\frac{1}{\ln 2}(2P_E)^{\left((m-1)|\ddot{D}_i|\right)}.\eta^{(m|\ddot{D}_i|-\varphi)}\sum_{\hat{l}=0}^{\xi}.\left[\left(\frac{\eta^{-(\varphi-\hat{l}-1)}}{\Gamma(\varphi)}\right)\right.\\ &\times\frac{1}{\eta}G_{4,3}^{2,3}\left(\frac{-\bar{\gamma}}{\eta}\middle|\begin{matrix}-\varphi+\hat{l}+1,1,1,0\\\hat{l},1,0\end{matrix}\right)\\ &\left.+\left(\frac{\phi.\eta^{\varphi-\hat{l}}}{\Gamma(\varphi+1)}\right).\frac{1}{\eta}G_{4,3}^{2,3}\left(\frac{-\bar{\gamma}}{\eta}\middle|\begin{matrix}-\varphi+\hat{l},1,1,0\\\hat{l},1,0\end{matrix}\right)\right] \qquad \text{(C-11)}\end{aligned}$$

REFERENCES

[1] O. E. Ijiga, R. Malekian, and U. A. K. Chude-Okonkwo, "Enabling emergent configurations in the industrial Internet of Things for oil and gas explorations: A survey," *Electronics*, vol. 9, no. 8, p. 1306, Aug. 2020.

[2] G. Kahyarara, "Maritime transport in Africa: Challenges, opportunities, and an agenda for future research," in *Proc. UNCTAD Ad Hoc Expert Meeting*, Sep. 2018, pp. 1–49.

[3] M. Manoufali, P.-Y. Kong, and S. Jimaa, "An overview of maritime wireless mesh communication technologies and protocols," *Int. J. Bus. Data Commun. Netw.*, vol. 10, no. 1, pp. 1–29, Jan. 2014.

[4] O. E. Ijiga, O. O. Ogundile, A. D. Familua, and D. J. J. Versfeld, "Review of channel estimation for candidate waveforms of next generation networks," *Electronics*, vol. 8, no. 9, p. 956, Aug. 2019.

[5] Y. Kim, Y. Song, and S. H. Lim, "Hierarchical maritime radio networks for internet of maritime things," *IEEE Access*, vol. 7, pp. 54218–54227, 2019.

[6] Y. Xu, "Quality of service provisions for maritime communications based on cellular networks," *IEEE Access*, vol. 5, pp. 23881–23890, 2017.

[7] H. Darvishi, D. Ciuonzo, E. R. Eide, and P. S. Rossi, "Sensor-fault detection, isolation and accommodation for digital twins via modular data-driven architecture," *IEEE Sensors J.*, vol. 21, no. 4, pp. 4827–4838, Feb. 2021.

[8] O. O. Ogundile, M. B. Balogun, O. E. Ijiga, and E. O. Falayi, "Energy-balanced and energy-efficient clustering routing protocol for wireless sensor networks," *IET Commun.*, vol. 13, no. 10, pp. 1449–1457, 2019.

[9] G. Roque and V. S. Padilla, "LPWAN based IoT surveillance system for outdoor fire detection," *IEEE Access*, vol. 8, pp. 114900–114909, 2020.

[10] D. Ciuonzo and P. Salvo Rossi, "Distributed detection of a non-cooperative target via generalized locally-optimum approaches," *Inf. Fusion*, vol. 36, pp. 261–274, Jul. 2017.

[11] T. Yang, Z. Zheng, H. Liang, R. Deng, N. Cheng, and X. Shen, "Green energy and content-aware data transmissions in maritime wireless communication networks," *IEEE Trans. Intell. Transp. Syst.*, vol. 16, no. 2, pp. 751–762, Apr. 2015.

[12] S.-W. Jo and W.-S. Shim, "LTE-maritime: High-speed maritime wireless communication based on LTE technology," *IEEE Access*, vol. 7, pp. 53172–53181, 2019.

[13] T. Mrkvička, M. Muška, and J. Kubečka, "Two step estimation for Neyman–Scott point process with inhomogeneous cluster centers," *Statist. Comput.*, vol. 24, no. 1, pp. 91–100, Jan. 2014.

[14] C. Saha, M. Afshang, and H. S. Dhillon, "Poisson cluster process: Bridging the gap between PPP and 3GPP HetNet models," in *Proc. Inf. Theory Appl. Workshop (ITA)*, Feb. 2017, pp. 1–9.

[15] B. Błaszczyszyn and D. Yogeshwaran, "Clustering comparison of point processes, with applications to random geometric models," in *Stochastic Geometry, Spatial Statistics and Random Fields*. Springer, 2015, pp. 31–71.

[16] J. Kopecký and T. Mrkvička, "On the Bayesian estimation for the stationary Neyman–Scott point processes," *Appl. Math.*, vol. 61, no. 4, pp. 503–514, Aug. 2016.

[17] G. K. Karagiannidis, N. C. Sagias, and P. T. Mathiopoulos, "$N*$Nakagami: A novel stochastic model for cascaded fading channels," *IEEE Trans. Commun.*, vol. 55, no. 8, pp. 1453–1458, Aug. 2007.

[18] G. K. Karagiannidis, T. A. Tsiftsis, and R. K. Mallik, "Bounds for multihop relayed communications in Nakagami-m fading," *IEEE Trans. Commun.*, vol. 54, no. 1, pp. 18–22, Jan. 2006.
[19] I. S. Gradshteyn and I. M. Ryzhik, *Table of Integrals, Series, and Products*, 6th ed. New York, NY, USA: Academic, 2000.
[20] S. S. Haykin, *Adaptive Filter Theory*. London, U.K.: Pearson, 2005.
[21] T. J. Rouphael, *RF and Digital SIGNAL Processing for Software-Defined Radio*. Amsterdam, The Netherlands: Elsevier, 2008.
[22] O. E. Ijiga, "Channel estimation techniques for filter bank multicarrier based transceivers for next generation of wireless networks," M.S. thesis, Univ. Witwatersrand, Johannesburg, South Africa, 2017.
[23] A. K. Jagannatham, "Estimation for wireless communications: MIMO/OFDM cellular and sensor networks," in *National Programmeon Technology Enhanced D Learning (NPTEL)*, Jan. 2016.
[24] Y. Zhao and A. Huang, "A novel channel estimation method for ofdm mobile communication systems based on pilot signals and transform-domain processing," in *Proc. IEEE 47th Veh. Technol. Conf. Technol. Motion*, vol. 3, May 1997, pp. 2089–2093.
[25] D. Schafhuber and G. Matz, "MMSE and adaptive prediction of time-varying channels for OFDM systems," *IEEE Trans. Wireless Commun.*, vol. 4, no. 2, pp. 593–602, Mar. 2005.
[26] Y. Chen, Y. Gu, and A. O. Hero, "Sparse LMS for system identification," in *Proc. IEEE Int. Conf. Acoust., Speech Signal Process.*, Apr. 2009, pp. 3125–3128.
[27] Z. Xu, F. Bai, and B. G. Zheng, "Improved variable ZA-LMS algorithm based on discrete cosine transform for high noise reduction," in *Proc. 35th Chin. Control Conf. (CCC)*, Jul. 2016, pp. 5116–5121.
[28] O. J. Tobias and R. Seara, "On the LMS algorithm with constant and variable leakage factor in a nonlinear environment," *IEEE Trans. Signal Process.*, vol. 54, no. 9, pp. 3448–3458, Sep. 2006.
[29] X. Wu and Z. Ma, "Modeling and performance analysis of cellular and device-to-device heterogeneous networks," in *Proc. IEEE Globecom Workshops (GC Wkshps)*, Dec. 2017, pp. 1–6.
[30] R. B. Manav and M. K. Arti, "On the closed-form performance analysis of maximal ratio combining in Shadowed–Rician fading LMS channels," *IEEE Commun. Lett.*, vol. 18, no. 1, pp. 54–57, Jan. 2014.
[31] A. Čolaković and M. Hadžialić, "Internet of Things (IoT): A review of enabling technologies, challenges, and open research issues," *Comput. Netw.*, vol. 144, pp. 17–39, Oct. 2018.
[32] G. A. Akpakwu, B. J. Silva, G. P. Hancke, and A. M. Abu-Mahfouz, "A survey on 5G networks for the Internet of Things: Communication technologies and challenges," *IEEE Access*, vol. 6, pp. 3619–3647, 2018.
[33] A. J. Onumanyi, A. M. Abu-Mahfouz, and G. P. Hancke, "Cognitive radio in low power wide area network for IoT applications: Recent approaches, benefits and challenges," *IEEE Trans. Ind. Informat.*, vol. 16, no. 12, pp. 7489–7498, Dec. 2020.

OWOICHO E. IJIGA (Member, IEEE) received the B.Eng. degree in electrical/electronic engineering from the Federal University of Agriculture, Makurdi, Nigeria, in 2012, the B.Eng. degree (Hons) in electronic engineering from the University of Pretoria, South Africa, in 2015, the Master of Science degree in electrical and information engineering from the University of the Witwatersrand, Johannesburg, South Africa, in 2017, and the Ph.D. degree in computer engineering from the University of Pretoria, in 2021. His research interests include channel estimation for filter bank multicarrier systems and industrial Internet of Things.

REZA MALEKIAN (Senior Member, IEEE) is currently an Extraordinary Professor with the Department of Electrical, Electronic and Computer Engineering, University of Pretoria, and also with the Department of Computer Science and Media Technology, Malmö University, Sweden. He is also registered as a Chartered Engineer with the Engineering Council of U.K. and a fellow of the British Computer Society. His research interests include advanced sensor networks and the Internet of Things. He is an Associate Editor of IEEE INTERNET OF THINGS JOURNAL, IEEE TRANSACTIONS ON INTELLIGENT TRANSPORTATION SYSTEMS, and *IET Networks*.

UCHE A. K. CHUDE-OKONKWO (Member, IEEE) received the Ph.D. degree from Universiti Teknologi Malaysia. He is currently a Senior Lecturer with the Institute of Intelligent Systems, University of Johannesburg, South Africa. His current research interests include molecular communication applied to advanced healthcare delivery, artificial intelligence, the IoT, complex systems, wireless communication, systems biology, and signal processing. He serves as a Technical Program Committee Member for IEEE GLOBECOM, and an Associate Editor for *Frontier in Communications and Networks* and the *SAIEE Africa Research Journal*.